E2-2003-99

G. N. Afanasiev, V. G. Kartavenko, Yu. P. Stepanovsky*

VAVILOV–CHERENKOV AND TRANSITION RADIATIONS ON THE DIELECTRIC AND METALLIC SPHERES

Submitted to «Journal of Mathematical Physics»

*Institute of Physics and Technology, Kharkov, Ukraine

1 Introduction

This paper has a twofold aim.
First, usually, a charge moves in one medium (1) while the measurements are made in another one (2). For example, in the original Cherenkov experiments [1], the electron moved in the vessel filled with water, while measurements were made outside this vessel, in air. The radiation of a charge moving inside the infinite cylindrical sample C was considered by Frank and Ginsburg [2] who shown that there is no radiation outside C if the Tamm-Frank radiation condition is not fulfilled there. It should be recalled that Frank and Ginsburg evaluated the energy flux in the direction perpendicular to the motion axis. The energy flux in the direction parallel to the motion axis was evaluated in [3]. It was shown there that this component of radiation is infinitely small for all frequencies except for the infinite discrete sequence of frequencies where it is infinite.
In the same reference [3], the geometrical optics consideration has been applied to the radiation of charge moving in the finite space interval lying completely inside the sphere S filled with a substance 1 with refractive index n_1. Observations are made outside S, in medium 2 with refractive index n_2. It was shown there that the angular spectrum broadens if $n_2 < n_1$. One of the goals of the present treatment is to make the quantitative analysis of this problem. For this, we evaluated angular and frequency radiation intensities for a number of charge velocities and media properties. In general, the presence of medium 2 outside S different from medium 1 inside S leads to the broadening of the angular spectrum and to the appearance of additional maxima at large angles. Calculations predict the oscillations of the frequency spectrum. This could be observed experimentally.

The second problem which will be studied here is the transition and Vavilov-Cherenkov (VC) radiations on the dielectric and metallic spheres. The notion of the transition radiation was introduced by Frank and Ginsburg [4] who studied radiation arising from the uniformly moving charge passing from one medium to another. They considered the plane boundary between media 1 and 2. A thorough exposition of the transition radiation may be found in [5]. In this consideration, we consider a charge motion which begins and terminates in medium 2 and which passes through the dielectric sphere filled with medium 1. The energy flux is evaluated in medium 2. As far as we know, the transition radiation only for plane interfaces was considered in physical literature. For the treated problem the angular and frequency radiation intensities are evaluated for a number of charge velocities and media properties. These expressions contain transition and VC radiations as well as the radiation from the charge instantaneous beginning and termination of motion. It is proved that the identification (frequently used by experimentalists) of the charge velocity by the Cherenkov radiation on the part of the charge trajectory where $\beta n > 1$ is not always valid in the presence of boundaries.

There are analysed also attempts to explain transition radiation in terms of the charge instantaneous termination of motion in one medium and the instantaneous charge beginning of motion in another medium. It is proved that their contribution to the radiation intensity disappears if the cnarge motion with instantaneous velocity jumps can be considered as a limiting case of the charge smooth motion. It is considered also the interpretation of the transition radiation in terms of semi-infinite charge motions with instantaneous termination of the charge motion in one medium and with its instantaneous

beginning of motion in the other one. It is shown that if the charge velocity is greater than the light velocity in medium, the terms corresponding to the VC radiation should be taken into account.

The plan of our exposition is as follows. The mathematical preliminaries are collected in Sec. 2. The expansion of the electromagnetic field in terms of Legendre polynomials for the Tamm problem is given in Sec. 3. In Sec. 4, a charge moving inside the dielectric sphere S filled with the substance 1 is considered. The radiation intensity is evaluated outside S, in medium 2. In Sec. 5, a charge whose motion begins and terminates in the medium 2 and which passes through the dielectric sphere filled with medium 1 or through the metallic one. The energy flux is evaluated in medium 2. In Sec. 6, the review of attempts to interpret the transition radiation in terms of sudden termination of the charge motion in one medium and its sudden beginning in the other one is given. A short resume of the results obtained is presented in Sec. 7.

2 Mathematical preliminaries

We consider the charge motion in medium as to be given and intend to evaluate the electromagnetic field arising from such a motion. The solving of Maxwell equations grounds on the use of the Green functions.

For the charge motion in medium with refractive index n, the Green function is equal to

$$G_n = \exp(ik_nR)/R, \quad R = |\vec{r} - \vec{r}'|.$$

Here $k_n = kn, k = \omega/c$ and n is the medium refractive index. Its expansion in spherical coordinates is given by (see, e.g. [6])

$$G_n = 2\sum_{m\geq 0} \epsilon_m (2l+1)\frac{(l-m)!}{(l+m)!}\cos m(\phi-\phi')G_l(r,r')P_l^m(\cos\theta)P_l^m(\cos\theta'), \qquad (2.2)$$

where

$$G_l(r,r') = ik_n j_l(k_n r_<)h_l(k_n r_>), \quad j_l(x) = \sqrt{\frac{\pi}{2x}}J_{l+1/2}(x), \quad h_l(x) = \sqrt{\frac{\pi}{2x}}H^{(1)}_{l+1/2}(x),$$

$\epsilon_m = 1/(1+\delta_{m,0})$; $r_> = r, r_< = r'$ if $r > r'$; $r_> = r', r_< = r$ if $r < r'$.

These equations are no longer valid if medium consists of two pieces with different refractive indices. We consider a particular case when space regions inside and outside the sphere S of the radius a are filled with the substances 1 and 2 with parameters ϵ_1, μ_1 and ϵ_2, μ_2, respectively. The Green function satisfying equations

$$(\triangle + k_1^2)G_n = -4\pi\delta^3(\vec{r} - \vec{r}')$$

for $r < a$ and

$$(\triangle + k_2^2)G_n = -4\pi\delta^3(\vec{r} - \vec{r}')$$

for $r > a$ has the same form as (2.2) but with $G_l(r,r')$ given by

$$G_l = ik_1\Theta(a-r)\Theta(a-r')j_l(k_1r_<)h_l(k_1r_>) + ik_2\Theta(r-a)\Theta(r'-a)j_l(k_2r_<)h_l(k_2r_>) +$$

$$+ik_1D_l\Theta(a-r)\Theta(r'-a)j_l(k_1r)h_l(k_2r') + ik_2C_l\Theta(r-a)\Theta(a-r')j_l(k_1r')h_l(k_2r). \quad (2.3)$$

Here $k_1 = kn_1$ and $k_2 = kn_2$ ($n_1 = \sqrt{\epsilon_1\mu_1}$ and $n_2 = \sqrt{\epsilon_2\mu_2}$ are the refractive indices of media 1 and 2, resp.). The constants C_l and D_l are defined by the boundary conditions at $r = a$.
The vector potential (VP) in the spectral representation for a charge moving along the z axis is found from the equation

$$A_z = \frac{1}{c}\int G(\vec{r},\vec{r}')\mu(r')j_z(\vec{r}')dV', \tag{2.4}$$

where $\mu = \mu_1$ for $r < a$ and $\mu = \mu_2$ for $r > a$. The integration is performed over space points where the spectral current density $j_z(\vec{r}')$ differs from zero.

3 Pedagogical example: the Tamm problem in a spherical basis

3.1 The original Tamm problem

Tamm considered the following problem [7]. A point charge is at rest at the point $z = -z_0$ of the z axis up to a moment $t = -t_0$ and at the point $z = z_0$ after the moment $t = t_0$. In the time interval $-t_0 < t < t_0$, it moves uniformly along the z axis with the velocity v greater than the light velocity in medium $c_n = c/n$. The nonvanishing z component of the VP in the spectral representation is given by

$$A_z(x,y,z) = \frac{e\mu}{2\pi c}\alpha_T, \tag{3.1}$$

where

$$\alpha_T = \int_{-z_0}^{z_0}\frac{dz'}{R}\exp\left[ik(\frac{z'}{\beta} + nR)\right], \quad R = [\rho^2 + (z-z')^2]^{1/2}, \quad \rho^2 = x^2 + y^2.$$

Imposing the conditions: i) $R >> z_0$ (this means that the observation distance is much larger than the motion interval); ii) $k_n R >> 1$, $k_n = \omega/c_n$ (this means that the observations are made in the wave zone); iii) $nz_0^2/2R\lambda << 1$, $\lambda = 2\pi c/\omega$ (this means that the second-order terms in the expansion of R should be small compared with π since they enter as a phase in (3.1); λ is the observed wavelength), Tamm obtained the following expression for the magnetic VP:

$$A_z = \frac{e\mu}{\pi n\omega r}\exp(iknr)q, \quad q = \frac{1}{1/\beta_n - \cos\theta}\sin[\frac{kLn}{2}(\frac{1}{\beta_n} - \cos\theta)]. \tag{3.2}$$

Here $L = 2z_0$ is the motion interval and $\beta_n = \beta n$. In the limit $kL \to \infty$, one gets

$$q \to \pi\delta(\frac{1}{\beta_n} - \cos\theta), \quad A_z \to \frac{e\mu}{\omega nr}\exp(iknr)\delta(\cos\theta - 1/\beta_n). \tag{3.3}$$

Using the vector potential (3.2), Tamm evaluated the electromagnetic field strengths and the energy flux through the sphere of the radius r for the whole time of observation

$$\mathcal{E} = R_0^2\int S_r d\Omega dt = \int\frac{d^2\mathcal{E}}{d\Omega d\omega}d\Omega d\omega, \quad d\Omega = \sin\theta d\theta d\phi, \quad S_r = \frac{c}{4\pi}E_\theta H_\phi$$

where

$$\frac{d^2\mathcal{E}}{d\Omega d\omega} = \frac{e^2\mu}{\pi^2 nc} q^2 \sin^2\theta \tag{3.4}$$

is the energy emitted into the solid angle $d\Omega$, in the frequency interval $d\omega$. This famous formula obtained by Tamm is frequently used by experimentalists for the identification of the charge velocity. Equation (3.4), being integrated over the solid angle, defines the frequency distribution of the radiation

$$\frac{d\mathcal{E}}{d\omega} = \int \frac{d^2\mathcal{E}}{d\Omega d\omega} d\Omega.$$

It is given by [8,9]

$$\begin{aligned}\frac{d\mathcal{E}}{d\omega} = \frac{2e^2\beta}{\pi c}(1-\frac{1}{\beta_n^2})\{&\frac{\sin^2[kL(1-\beta_n)/2\beta]}{1-\beta_n} - \frac{\sin^2\omega[kL(1+\beta_n)/2\beta]}{1+\beta_n} \\ &-\frac{kL}{2\beta}[si(\frac{kL}{\beta}(1-\beta_n)) - si(\frac{kL}{\beta}(1+\beta_n))]\}- \\ -\frac{2e^2}{\pi cn^2\beta}&[\ln\frac{|1-\beta_n|}{1+\beta_n} - ci(\frac{kL}{\beta}|1-\beta_n|) + ci(\frac{kL}{\beta}(1+\beta_n))]- \\ -\frac{e^2}{\pi cn^2}&\{2n + \frac{1}{kL}[\sin(\frac{kL}{\beta}(1-\beta_n)) - \sin(\frac{kL}{\beta}(1+\beta_n))]\}.\end{aligned} \tag{3.5}$$

Here $si(x)$ and $ci(x)$ are the integral sine and cosine defined by equations

$$si(x) = -\int_x^\infty \frac{\sin t}{t} dt, \quad ci(x) = -\int_x^\infty \frac{\cos t}{t} dt.$$

For $kL >> 1$, Eq.(3.5) reduces to the form given by Tamm:

$$\frac{d\mathcal{E}}{d\omega} = W_{BS} \tag{3.6}$$

for $v < c_n$ and

$$\frac{d\mathcal{E}}{d\omega} = W_{BS} + W_{Ch} \tag{3.7}$$

for $v > c_n$. Here

$$W_{BS} = \frac{2e^2\mu}{\pi c\beta n^2}(\ln\frac{1+\beta_n}{|1-\beta_n|} - 2\beta_n) \quad \text{and} \quad W_{Ch} = \frac{e^2\mu kL}{c}(1-\frac{1}{\beta_n^2}).$$

Tamm identified W_{BS} with the spectral distribution of the bremsstrahlungs, arising from the charge instantaneous acceleration and deceleration at the moments $\pm t_0$, resp. On the other hand, W_{Ch} was identified with the spectral distribution of the VC radiation. This is supported by the fact that W_{Ch} related to the charge motion interval coincides with the famous Frank-Tamm formula describing the energy radiated per unit length and per unit frequency for the charge unbounded motion [10]

$$\frac{d^2\mathcal{E}}{d\omega dL} = \frac{e^2}{c^2}(1-\frac{1}{\beta_n^2}).$$

The typical experimental situations described by the Tamm formula are: i) the β decay of a nucleus at one space point accompanied by a subsequent absorption of the emitted electron at another point; ii) A high energy electron consequently moves in vacuum, enters into the dielectric slab, leaves the slab and propagates again in vacuum. Since the electron moving uniformly in vacuum does not radiate (apart from the transition radiation arising at the boundaries of the dielectric slab), the experimentalists describe this situation via the Tamm formula, assuming that the electron is created at one side of the slab and is absorbed at the other (see, e.g., [8,11-15]).

3.2 Expansion of the Tamm problem in terms of Legendre polynomials

Let a charge moves in medium in a finite interval $(-z_0, z_0)$ (this corresponds to the so-called Tamm problem). Then, the current density corresponding to the Tamm problem, in the spherical coordinates, is given by

$$j_z(\omega) = \frac{e}{4\pi^2 r^2 \sin\theta}[\delta(\theta)\exp(\frac{ikr}{\beta}) + \delta(\theta-\pi)\exp(-\frac{ikr}{\beta})]\Theta(z_0 - r). \tag{3.8}$$

Then, using (2.2), one gets on the observation sphere of the radius $r > z_0$,

$$A_z(\omega) = \frac{ie\mu kn}{2\pi c}\sum(2l+1)P_l h_l(knr)J_l(0,z_0),$$

$$H_\phi(\omega) = -\frac{iek^2n^2}{2\pi c}\sum P_l^1 h_l(knr)\tilde{J}_l(0,z_0), \quad E_\theta(\omega) = -\frac{ek^2\mu n}{2\pi c}\sum P_l^1 H_l(knr)\tilde{J}_l(0,z_0). \tag{3.9}$$

Here

$$J_l(0,z_0) = \int_0^{z_0} j_l(knr')f_l(r')dr', \quad \tilde{J}_l(0,z_0) = J_{l-1}(0,z_0) + J_{l+1}(0,z_0),$$

$$H_l(x) = \dot{h}_l(x) + \frac{h_l(x)}{x}.$$

$$f_l(r') = \exp(\frac{ikr'}{\beta}) + (-1)^l\exp(-\frac{ikr'}{\beta}), \quad k_1 = kn_1, \quad k_2 = kn_2.$$

In obvious cases, we omit the arguments of the Legendre polynomials if they equal $\cos\theta$. At large distances ($kr >> 1$) one can replace Hankel functions by their asymptotic values:

$$A_z \sim \frac{e\mu}{2\pi cr}\exp(iknr)\sum(2l+1)i^{-l}P_l J_l(0,z_0),$$

$$H_\phi \sim -\frac{ekn}{2\pi cr}\exp(iknr)\sum i^{-l}P_l^1\tilde{J}_l(0,z_0), \quad E_\theta \sim -\frac{ek\mu}{2\pi cr}\exp(iknr)\sum i^{-l}P_l^1\tilde{J}_l(0,z_0).$$

The angular radiation intensity on the sphere of the radius r

$$\frac{d^2\mathcal{E}}{d\omega d\Omega} = \frac{1}{2}cr^2(E_\theta H_\phi^* + c.c.) = \frac{e^2k^2n\mu}{4\pi^2 c}|\sum i^{-l}P_l^1\tilde{J}_l(0,z_0)|^2 =$$

$$= \frac{e^2k^2n\mu\sin^2\theta}{4\pi^2c}|\sum(2l+1)i^{-l}P_lJ_l(0,z_0)|^2. \tag{3.10}$$

Or, in a manifest form,

$$\frac{d^2\mathcal{E}}{d\omega d\Omega} = \frac{e^2\mu n}{\pi^2 c}\sin^2\theta(S_1+S_2)^2. \tag{3.11}$$

where

$$S_1 = \sum_{l=0}^{\infty}(-1)^l(4l+1)P_{2l}(\cos\theta)I^c_{2l}, \quad S_2 = \sum_{l=0}^{\infty}(-1)^l(4l+3)P_{2l+1}(\cos\theta)I^s_{2l+1},$$

$$I^c_{2l} = \int_0^{kz_0} j_{2l}(nx)\cos(\frac{x}{\beta})dx, \quad I^s_{2l+1} = \int_0^{kz_0} j_{2l+1}(nx)\sin(\frac{x}{\beta})dx. \tag{3.12}$$

Integrating (3.11) over the solid angle, one obtains the frequency distribution of the radiation:

$$\frac{d\mathcal{E}}{d\omega} = \frac{e^2k^2n\mu}{\pi c}|\sum\frac{l(l+1)}{2l+1}|\tilde{J}_l(0,z_0)|^2 =$$

$$= \frac{8e^2n\mu}{\pi c}[\sum\frac{(l+1)(2l+1)}{4l+3}(I^c_{2l}+I^c_{2l+2})^2 + \sum\frac{l(2l+1)}{4l+1}(I^s_{2l+1}+I^s_{2l-1})^2]. \tag{3.13}$$

These equations are valid if the radius r of the observation sphere is larger than z_0.

Numerical calculations show that Eqs. (3.11) and (3.13) coincide with the corresponding Tamm equations (3.4) and (3.5).

We concentrate now on the vector potential. For this, we rewrite it as

$$A_z = \frac{ie\mu n}{\pi c}\sum_{l=0}^{\infty}(4l+1)h_{2l}(knr)P_{2l}(\cos\theta)I^c_{2l} - \frac{e\mu n}{\pi c}\sum_{l=0}^{\infty}(4l+3)h_{2l+1}(knr)P_{2l+1}(\cos\theta)I^s_{2l+1}. \tag{3.14}$$

Usually, observations are made on large distances. For example, for $\lambda = 4\cdot 10^{-5}cm$ and $r = 1m$, $kr = 2\pi r/\lambda \sim 10^7$. Replacing the Hankel functions by their asymptotic values, one gets

$$A_z = \frac{e\mu}{kr\pi c}\exp(iknr)(S_1+S_2). \tag{3.15}$$

Obviously, (3.2) and (3.15) should coincide (since the same assumptions are involved in their derivation). Equating them, one gets

$$S_1+S_2 = \frac{1}{n}\frac{\sin[kz_0n(\cos\theta - 1/\beta_n)}{\cos\theta - 1/\beta_n}. \tag{3.16}$$

Now we consider the coefficients I^c_{2l} and I^s_{2l+1}. In the limit $kz_0 \to \infty$, the integrals

$$I^c_{2l} = \int_0^{\infty} j_{2l}(nx)\cos(\frac{x}{\beta})dx, \quad I^s_{2l+1} = \int_0^{\infty} j_{2l+1}(nx)\sin(\frac{x}{\beta})dx$$

can be evaluated in a closed form (see, e.g., [6]). They are given 0 for $\beta n < 1$ and

$$I^c_{2l} = \frac{\pi}{2n}(-1)^l P_{2l}(1/\beta n), \quad I^s_{2l+1} = \frac{\pi}{2n}(-1)^l P_{2l+1}(1/\beta n)$$

for $\beta n > 1$. Substituting this into (3.15), one gets

$$A_\omega = \frac{e\mu}{2nkrc}\exp(iknr)\times$$

$$\times[\sum_{l=0}^{\infty}(4l+1)P_{2l}(\cos\theta)P_{2l}(1/\beta n) + \sum_{l=0}^{\infty}(4l+3)P_{2l+1}(\cos\theta)P_{2l+1}(1/\beta n)] =$$

$$= \frac{e\mu}{2nkrc}\exp(iknr)\sum_{l=0}^{\infty}(2l+1)P_l(\cos\theta)P_l(1/\beta n) = \frac{e\mu}{nkrc}\exp(iknr)\delta(\cos\theta - 1/\beta n). \quad (3.17)$$

In deriving this, we used the completeness relation

$$\sum_{l=0}^{\infty}(l+1/2)P_l(x)P_l(x') = \delta(x-x').$$

Vector potential (3.17) coincides with the one entering into (3.3).

4 The Tamm problem for a charge moving inside the spherical sample

4.1 Main formulae

Let a charge move in a finite space interval $(-z_0, z_0)$ lying entirely inside the sphere S of the radius a (FIG. 1). The sphere is filled by a substance 1 with parameters ϵ_1 and μ_1.

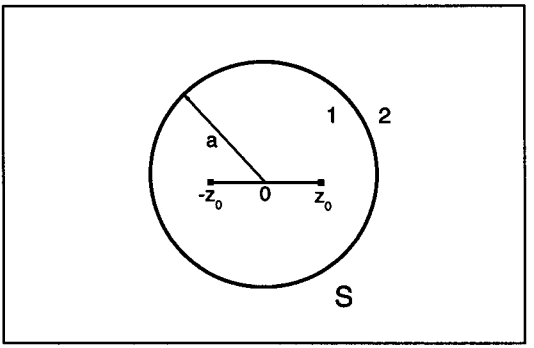

Figure 1: A charge moves inside the dielectric sphere S filled with the medium 1. The radiation of intensity is measured outside S, in medium 2.

The observations are made in the medium 2 with parameters ϵ_2 and μ_2 surrounding S. The EMF strengths contributing to the radial energy flux are equal to (see Appendix 1)

$$H_\phi = -\frac{iek^2n_2^2}{2\pi c}\sum \tilde{C}_l P_l^1 h_l(k_2 r),$$

$$E_\theta = -\frac{i}{\epsilon_2 kr}\frac{d}{dr}(rH_\phi) = -\frac{e\mu_2 n_2 k^2}{2\pi c}\sum H_l(k_2 r)P_l^1\tilde{C}_l \tag{4.1}$$

for $r > a$ and

$$H_\phi = -\frac{iek^2 n_1^2}{2\pi c}\sum P_l^1[\tilde{D}_l j_l(k_1 r) + \tilde{J}_l^{(1)}(0,z_0)h_l(k_1 r)],$$

$$E_\theta = -\frac{e\mu_1 n_1 k^2}{2\pi c}\sum P_l^1[\tilde{D}_l J_l(k_1 r) + \tilde{J}_l^{(1)}(0,z_0)H_l(k_1 r)] \tag{4.2}$$

for $z_0 < r < a$. Here

$$\tilde{J}_l^{(1)}(x,y) = J_{l-1}^{(1)}(x,y) + J_{l+1}^{(1)}(x,y), \quad J_l^{(1)}(x,y) = \int_x^y j_l(k_1 r')f_l(r')dr',$$

$$J_l(x) = \frac{dj_l(x)}{dx} + \frac{j_l(x)}{x} = \frac{1}{2l+1}[(l+1)j_{l-1} - lj_{l+1}],$$

$$H_l(x) = \frac{dh_l(x)}{dx} + \frac{h_l(x)}{x} = \frac{1}{2l+1}[(l+1)h_{l-1} - lh_{l+1}].$$

Imposing the continuity of H_ϕ and E_θ at $r = a$, one finds the following equations for $\tilde{C}_l$ and $\tilde{D}_l$:

$$n_2^2\tilde{C}_l h_l(2) - n_1^2\tilde{D}_l j_l(1) = n_1^2 h_l(1)\tilde{J}_l^{(1)}(0,z_0),$$

$$\mu_2 n_2\tilde{C}_l H_l(2) - \mu_1 n_1\tilde{D}_l J_l(1) = \mu_1 n_1 H_l(1)\tilde{J}_l^{(1)}(0,z_0), \tag{4.3}$$

where $1 = k_1 a$ and $2 = k_2 a$. From this one easily finds $\tilde{C}_l$:

$$\tilde{C}_l = \frac{i\mu_1}{n_2 k^2 a^2 \triangle_l}\tilde{J}_l^{(1)}(0,z_0), \tag{4.4}$$

where

$$\triangle_l = \mu_2 n_1 j_l(1)H_l(2) - \mu_1 n_2 J_l(1)h_l(2).$$

At large distances ($kr >> 1$) one can replace Hankel function by its asymptotic value. Then,

$$H_\phi = -\frac{ekn_2}{2\pi c}\frac{\exp(ik_2 r)}{r}S, \quad E_\theta = -\frac{ek\mu_2}{2\pi c}\frac{\exp(ik_2 r)}{r}S, \tag{4.5}$$

where

$$S = \sum i^{-l}P_l^1\tilde{C}_l. \tag{4.6}$$

The radiation intensity per unit frequency unit and per unit solid angle is

$$\frac{d^2\mathcal{E}}{d\Omega d\omega} = \frac{1}{2}cr^2(E_\theta H_\phi^* + c.c.) = \frac{e^2k^2 n_2\mu_2}{4\pi^2 c}|S|^2. \tag{4.7}$$

The integration over the solid angle gives the frequency distribution of radiation

$$\frac{d\mathcal{E}}{d\omega} = \frac{e^2k^2 n_2\mu_2}{\pi c}\sum\frac{l(l+1)}{2l+1}|\tilde{C}_l|^2. \tag{4.8}$$

When the media inside and outside S are the same ($\epsilon_1 = \epsilon_1 = \epsilon$, $\mu_1 = \mu_2 = \mu$), one gets

$$\Delta_l = \frac{i\mu}{nk^2a^2} \quad \text{and} \quad \tilde{C}_l = \tilde{J}_l^{(1)}(0,z_0),$$

that is, one arrives at the one-medium Tamm problem for the space interval $(-z_0, z_0)$.

4.2 Numerical results

In FIG. 2, there are shown angular radiation intensities (solid lines) evaluated according (4.7) for $kz_0 = 10, \quad ka = 20, n_1 = 2$ and $n_2 = 1$ (that is, there is a vacuum outside S) for a number of charge velocities. Side by side with them, the Tamm angular intensities (3.4) (dotted lines) corresponding to $n = n_1, L = 2z_0$ are shown. The distinction of (4.7) from (3.4) is due to the presence of the medium 2 outside S not coinciding with medium 1. This results in the broadening of the angular intensity distribution and in its rise at large observation angles.

The corresponding frequency distributions (4.8) (solid lines) together with the Tamm frequency distributions (3.5) (dotted lines) are shown in FIG. 3. It is seen that the frequency distribution (4.8) oscillates around the the Tamm one (3.5). When evaluating $d\mathcal{E}/d\omega$, we implicitly assumed that the refractive index n_1 does not depend on ω in the treated frequency interval. In fact, this is a common thing in refractive media. For example, for the usual water the refractive index is almost constant in the frequency interval $6 \cdot 10^{14} < \omega < 6 \cdot 10^{15} s^{-1}$ encompassing the visible light region. In FIG. 4, there are shown angular radiation intensities (solid lines) evaluated according (4.7) for $kz_0 = 10, \quad ka = 20, n_1 = 1$ and $n_2 = 2$ (that is, there is a vacuum inside S) for a number of charge velocities. Side by side with them, the Tamm angular intensities (3.4) (dotted lines) corresponding to $n = n_1, L = 2z_0$ are shown. It is seen that the presence of medium outside S affects not so strongly as in FIG. 2.

The corresponding frequency distributions are shown in FIG. 5. Again, oscillations around the Tamm frequency distribution (3.5) are observed.

Probably, the rise of angular intensities at large angles shown in FIGS. 2 and 4 is due to the reflection of the VC radiation from the internal side of S

5 The Tamm problem for a charge passing through the sphere

5.1 Dielectric sphere

5.1.1 Main formulae

Let a charge move with a constant velocity v in the interval $(-z_0, z_0)$. There is a sphere S of the radius $a < z_0$ with its center at the origin (FIG. 6). The space inside S is filled by the substance with parameters ϵ_1, μ_1. Outside S there is substance with parameters ϵ_2, μ_2. The EMF strengths contributing to the radial energy flux are (see Appendix 2)

$$H_\phi = -\frac{iek_2^2}{2\pi c} \sum \tilde{C}_l P_l^1 h_l(k_2 r), \quad E_\theta = -\frac{ek^2 \mu_2 n_2}{2\pi c} \sum H_l(k_2 r) P_l^1 \tilde{C}_l \tag{5.1}$$

for $r > z_0$,

$$H_\phi = -\frac{iek_2^2}{2\pi c} \sum \tilde{P}_l^1 [\tilde{C}_l h_l(k_2 r) - h_l(k_2 r) \tilde{J}_l^{(2)}(r, z_0) + j_l(k_2 r) \tilde{H}_l^{(2)}(r, z_0)],$$

$$E_\theta = -\frac{ek^2 \mu_2 n_2}{2\pi c} \sum \tilde{P}_l^1 [\tilde{C}_l H_l(k_2 r) - H_l(k_2 r) \tilde{J}_l^{(2)}(r, z_0) + J_l(k_2 r) \tilde{H}_l^{(2)}(r, z_0)] \tag{5.2}$$

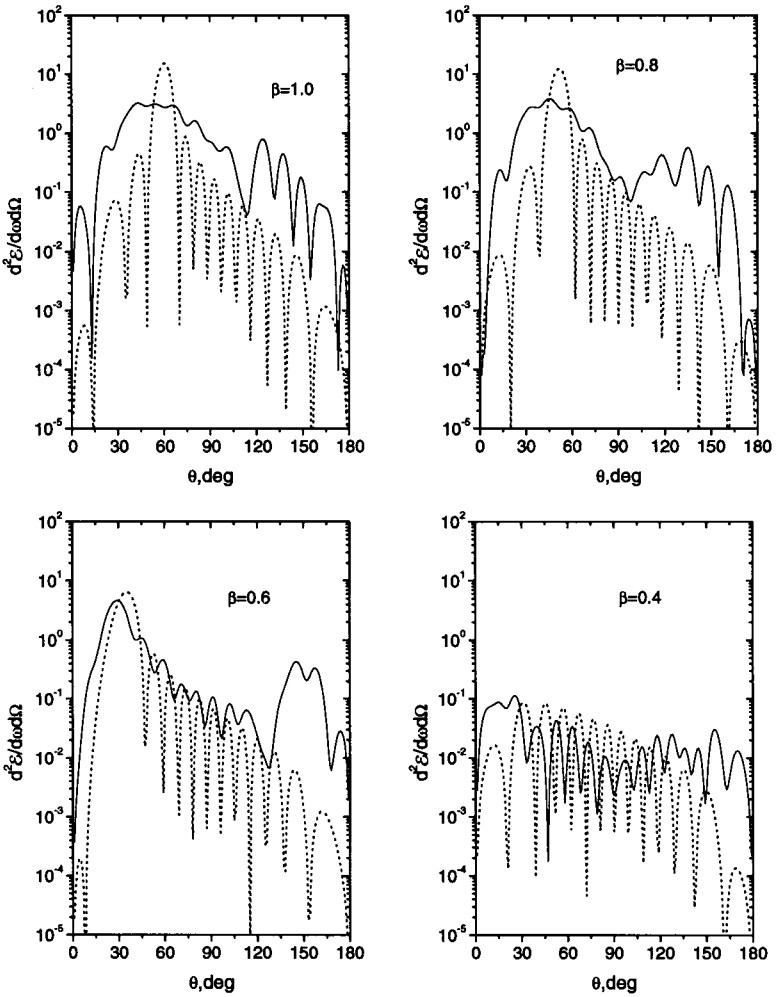

Figure 2: Angular radiation intensities in e^2/c units (solid curves) for the charge motion shown in FIG. 1 and various charge velocities. The media parameters are $n_1 = 2, n_2 = 1$ (that is, there is vacuum outside the sphere S). Further, $kz_0 = 10, ka = 20$. The dotted curves are the Tamm angular intensities (3.4) evaluated for $kL = 2kz_0$ and $n = n_1$. The difference between these two curves is due to the fact that the medium outside S is not the same as inside S. The exact angular intensities are much broader than the corresponding Tamm ones. Probably, the rise of angular intensities at large angles is due to the reflection of the VC radiation from the internal side of S.

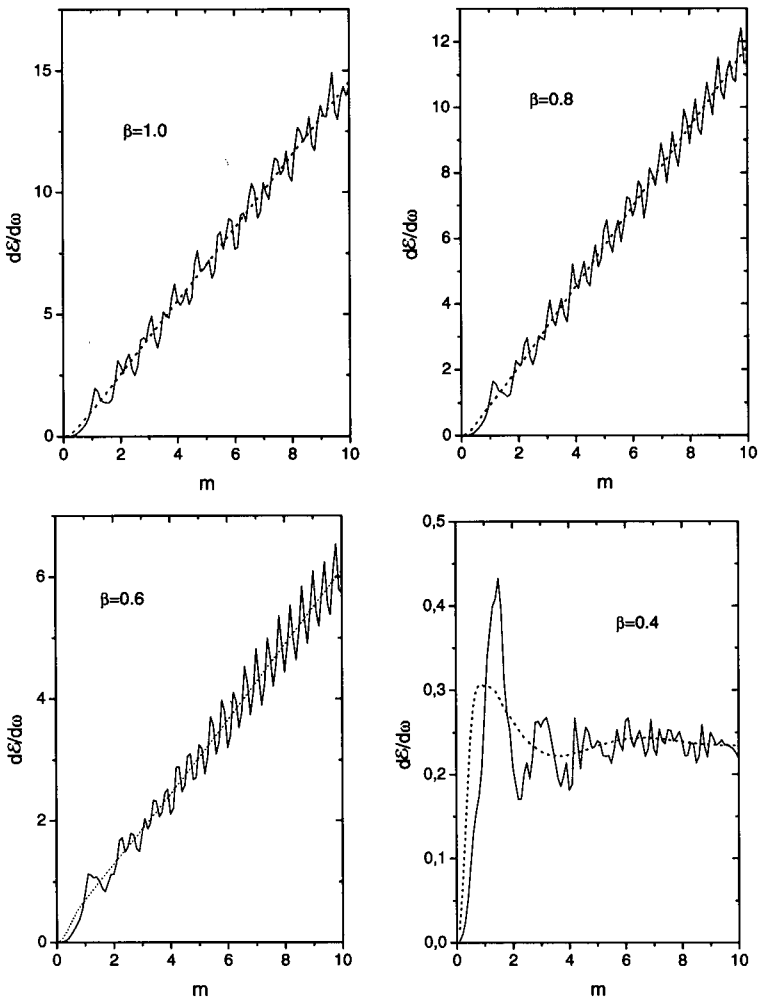

Figure 3: Frequency radiation intensities in e^2/c units (solid curves) for the charge motion shown in FIG. 1 and various charge velocities. The media parameters are the same as in FIG. 2. Further, $kz_0 = m, ka = 2m$. The dotted curves are the Tamm frequency intensities (3.5) evaluated for $kL = 2kz_0$ and $n = n_1$. It is seen that frequency intensities (4.8) oscillate around the Tamm ones.

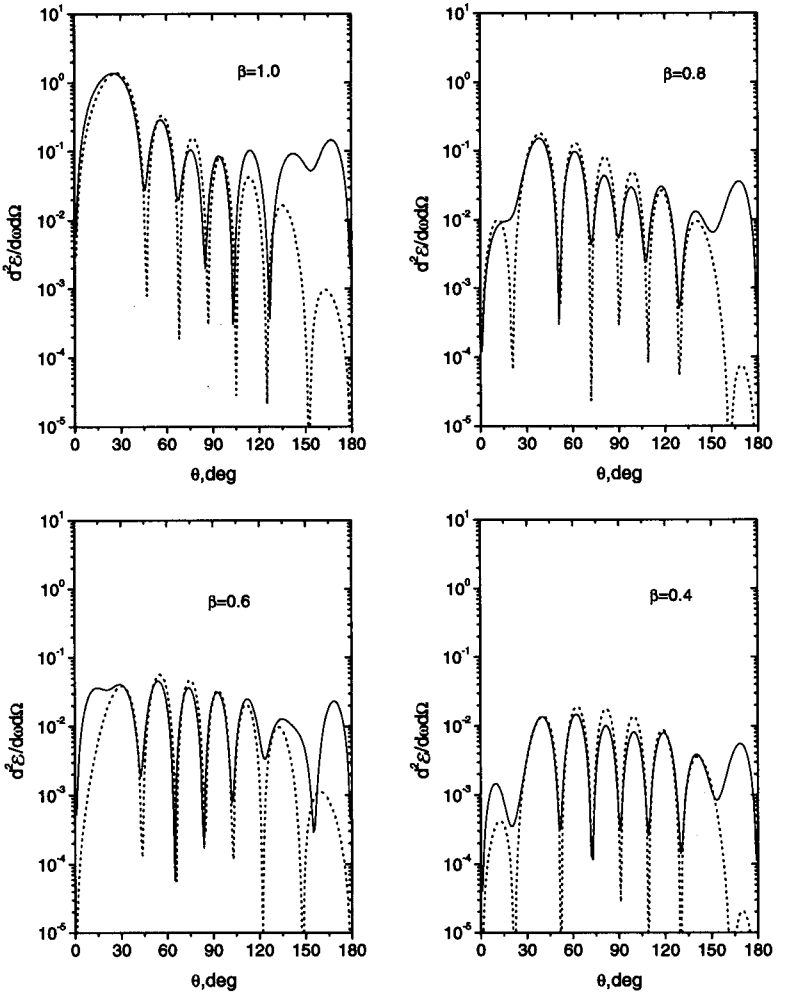

Figure 4: The same as in Fig.2 but for $n_1 = 1, n_2 = 2$ (that is, there is vacuum inside S). The dotted curves are the Tamm angular intensities (3.4) evaluated for $kL = 2kz_0$ and $n = n_1$.

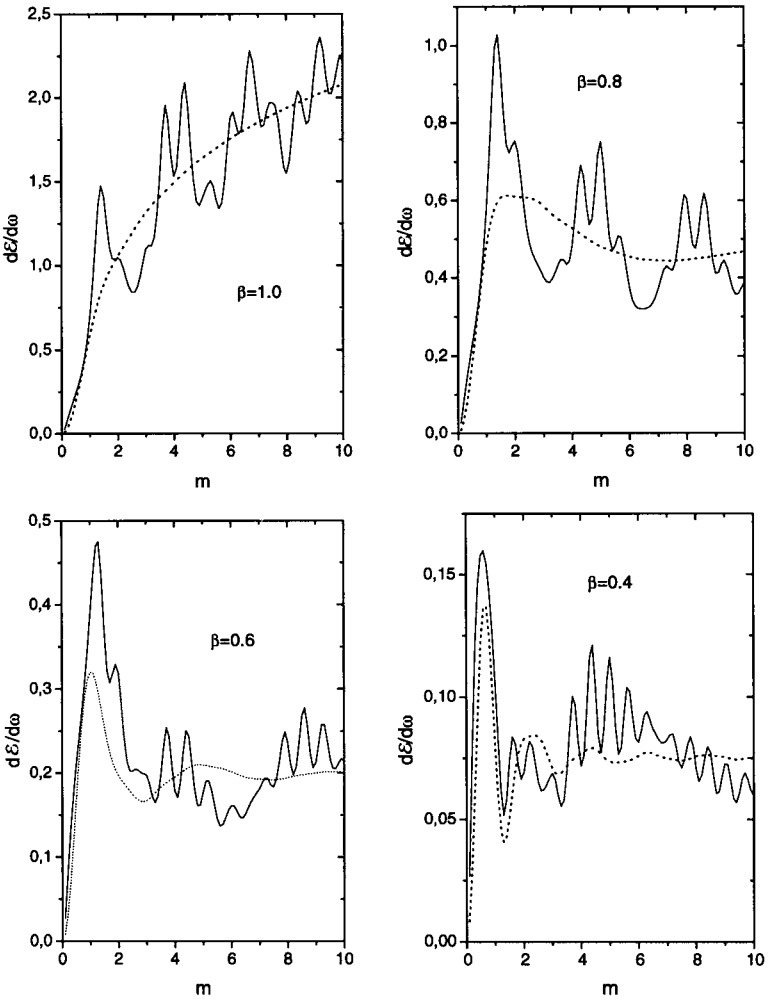

Figure 5: The same as in Fig. 3 but for $n_1 = 1, n_2 = 2$ (vacuum inside S). The Tamm frequency intensities (3.5) are evaluated for $kL = 2kz_0$ and $n = n_1$.

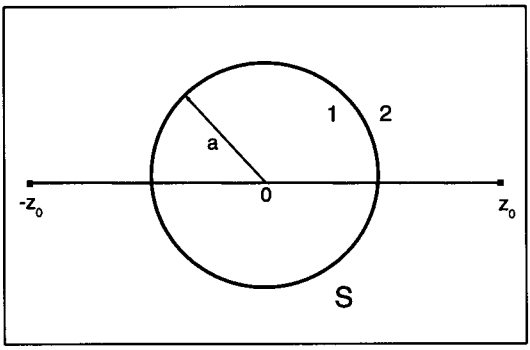

Figure 6: A charge motion begins and terminates in medium 2. It passes through sphere S filled with the medium 1. The radiation of intensity is measured outside S, in medium 2.

for $a < r < z_0$ and

$$H_\phi = -\frac{iek_1^2}{2\pi c}\sum \tilde{P}_l^1[\tilde{D}_l j_l(k_1 r) + h_l(k_1 r)\tilde{J}_l^{(1)}(0,r) + j_l(k_1 r)\tilde{H}_l^{(1)}(r,a)],$$

$$E_\theta = -\frac{ek^2\mu_1 n_1}{2\pi c}\sum \tilde{P}_l^1[\tilde{D}_l J_l(k_1 r) + H_l(k_1 r)\tilde{J}_l^{(1)}(0,r) + J_l(k_1 r)\tilde{H}_l^{(1)}(r,a)] \qquad (5.3)$$

for $r < a$. Here

$$\tilde{H}_l^{(1)}(x,y) = H_{l-1}^{(1)}(x,y) + H_{l+1}^{(1)}(x,y), \quad \tilde{J}_l^{(2)}(x,y) = J_{l-1}^{(2)}(x,y) + J_{l+1}^{(2)}(x,y),$$

$$\tilde{H}_l^{(2)}(x,y) = H_{l-1}^{(2)}(x,y) + H_{l+1}^{(2)}(x,y), \quad H_l^{(1)}(x,y) = \int_x^y h_l(k_1 r')f_l(r')dr',$$

$$J_l^{(2)}(x,y) = \int_x^y j_l(k_2 r')f_l(r')dr' \quad H_l^{(2)}(x,y) = \int_x^y h_l(k_2 r')f_l(r')dr.'$$

Equating E_θ and H_ϕ at $r = a$, one obtains the following equations for $\tilde{C}_l$ and $\tilde{D}_l$:

$$n_2^2 h_l(2)\tilde{C}_l - n_1^2 j_l(1)\tilde{D}_l =$$

$$= n_1^2 h_l(1)\tilde{J}_l^{(1)}(0,a) + n_2^2[h_l(2)\tilde{J}_l^{(2)}(a,z_0) - j_l(2)\tilde{H}_l^{(2)}(a,z_0)],$$

$$\mu_2 n_2 H_l(2)\tilde{C}_l - \mu_1 n_1 J_l(1)\tilde{D}_l =$$

$$= \mu_1 n_1 H_l(1)\tilde{J}_l^{(1)}(0,a) + n_2\mu_2[H_l(2)\tilde{J}_l^{(2)}(a,z_0) - J_l(2)\tilde{H}_l^{(2)}(a,z_0)]. \qquad (5.4)$$

Here we put $1 = k_1 a$ and $2 = k_2 a$. For example, $j_l(1) \equiv j_l(k_1 a)$, etc. From this one easily obtains $\tilde{C}_l$:

$$\tilde{C}_l = \frac{1}{\Delta_l}\{\frac{i\mu_1}{n_2 k^2 a^2}\tilde{J}_l^{(1)}(0,a) + \tilde{J}_l^{(2)}(a,z_0)[\mu_2 n_1 j_l(1)H_l(2) - \mu_1 n_2 J_l(1)h_l(2)] -$$

$$-\tilde{H}_l^{(2)}(a,z_0)[\mu_2 n_1 j_l(1)J_l(2)-\mu_1 n_2 J_l(1)j_l(2)]\}=$$

$$=\frac{i}{\triangle_l}\{\frac{\mu_1}{n_2k^2a^2}\tilde{J}_l^{(1)}(0,a)+\tilde{J}_l^{(2)}(a,z_0)[\mu_2 n_1 j_l(1)N_l(2)-\mu_1 n_2 J_l(1)n_l(2)]-$$

$$-\tilde{N}_l^{(2)}(a,z_0)[\mu_2 n_1 j_l(1)J_l(2)-\mu_1 n_2 J_l(1)j_l(2)]\}. \tag{5.5}$$

Here $\triangle_l = n_1\mu_2 j_l(1)H_l(2)-\mu_1 n_2 J_l(1)h_l(2)$. At large distances ($kr >> 1$), one has

$$H_\phi \approx -\frac{ekn_2}{2\pi cr}\exp(ikn_2 r)S, \quad E_\theta \approx -\frac{ek\mu_2}{2\pi cr}\exp(ikn_2 r)S, \tag{5.6}$$

where

$$S=\sum i^{-l}\tilde{C}_l P_l^1. \tag{5.7}$$

Correspondingly, the energy flux through the sphere of the radius r is

$$\frac{d^2\mathcal{E}}{d\omega d\Omega}=\frac{1}{2}cr^2(E_\theta H_\phi^* + c.c.)=\frac{e^2k^2n_2\mu_2}{4\pi^2 c}|S|^2. \tag{5.8}$$

Integration over the solid angle gives the frequency distribution of radiation

$$\frac{d\mathcal{E}}{d\omega}=\frac{e^2k^2n_2\mu_2}{\pi c}\sum\frac{l(l+1)}{2l+1}|\tilde{C}_l|^2. \tag{5.9}$$

The one-medium Tamm problem is obtained either in the limit $ka \to 0$ or when media 1 and 2 are the same.

5.1.2 Numerical results

In FIG. 7, there are shown angular radiation intensities (solid lines) evaluated according (5.8) for $kz_0 = 20$, $ka = 10, n_1 = 2$ and $n_2 = 1$ (that is, there is a vacuum outside the sphere S and a substance with $n_1 = 2$ inside it) for a number of charge velocities. Side by side with them, the Tamm angular intensities (3.4) (dotted lines) corresponding to $n = n_1, L = 2a$ are shown. It is the usual thing in the VC radiation theory to associate the observed radiation with the part of the charge trajectory where $\beta n > 1$ (see, e.g., [10] and (ii) item at the end of subsection (III.A)). It the treated case, it lies within the sphere S. We observe a rather poor agreement of the exact intensity (5.8) with the Tamm one (3.4). Experimentalist studying, e.g., electron passing through the dielectric sphere S, will not see the pronounced Cherenkov maximum at $\theta = \theta_c$ ($\cos\theta_c = 1/\beta n$) and, on these grounds, will not identify the charge velocity. For $\beta = 0.4$ we did not present the Tamm intensity since for this velocity the Tamm intensities arising from the charge motion in $0 < r < a$ (medium 1) and $a < r < z_0$ (medium 2) intervals are of the same order. It is not clear to us how to combine the corresponding Tamm amplitudes. In any case, Eqs. (5.8) and (5.9) give the exact solution of the treated problem, while the Tamm intensities are needed only for the interpretation purposes. The corresponding frequency distribution (5.9) also differs appreciably from the Tamm one (3.5) (FIG. 8).

In FIG. 9, there are shown angular radiation intensities (solid lines) evaluated according (5.2) for $kz_0 = 20$, $ka = 10, n_1 = 1$ and $n_2 = 2$ (that is, the vacuum bubble inside S surrounded by a substance with $n_2 = 2$) for a number of charge velocities. Side by side with them, the Tamm angular intensities (3.4) (dotted lines) corresponding to

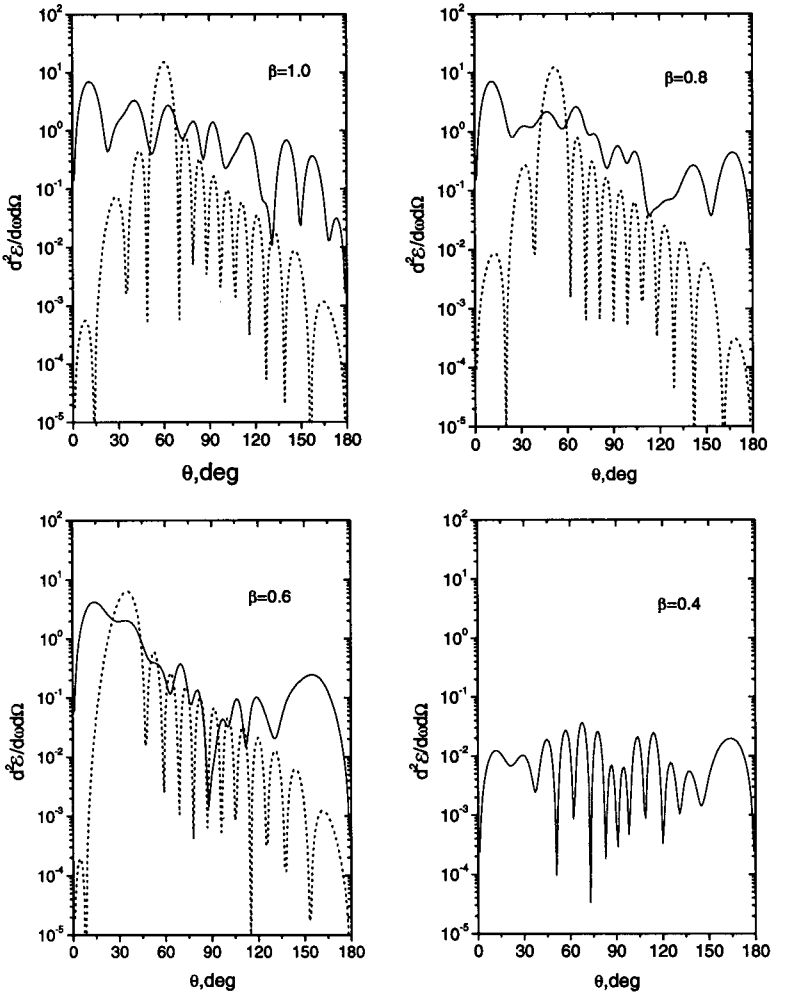

Figure 7: Angular radiation intensities in e^2/c units (solid curves) for the charge motion shown in FIG. 6 and various charge velocities. The medium inside S is dielectric with $n_1 = 2$. Outside S there is vacuum ($n_2 = 1$). Further, $ka = 10, kz_0 = 20$. The dotted curves are the Tamm angular intensities (3.4) evaluated for $kL = 2ka$ and $n = n_1$. The noncoincidence of exact angular intensities with the corresponding Tamm ones and, in particular, the absence of the pronounced maximum at $\cos\theta = 1/\beta n$ (especially for $\beta = 1$ and $\beta = 0.8$) demonstrates that the applicability of the Tamm formula for describing the radiation arising from the charge passage through the dielectric sample is rather limited.

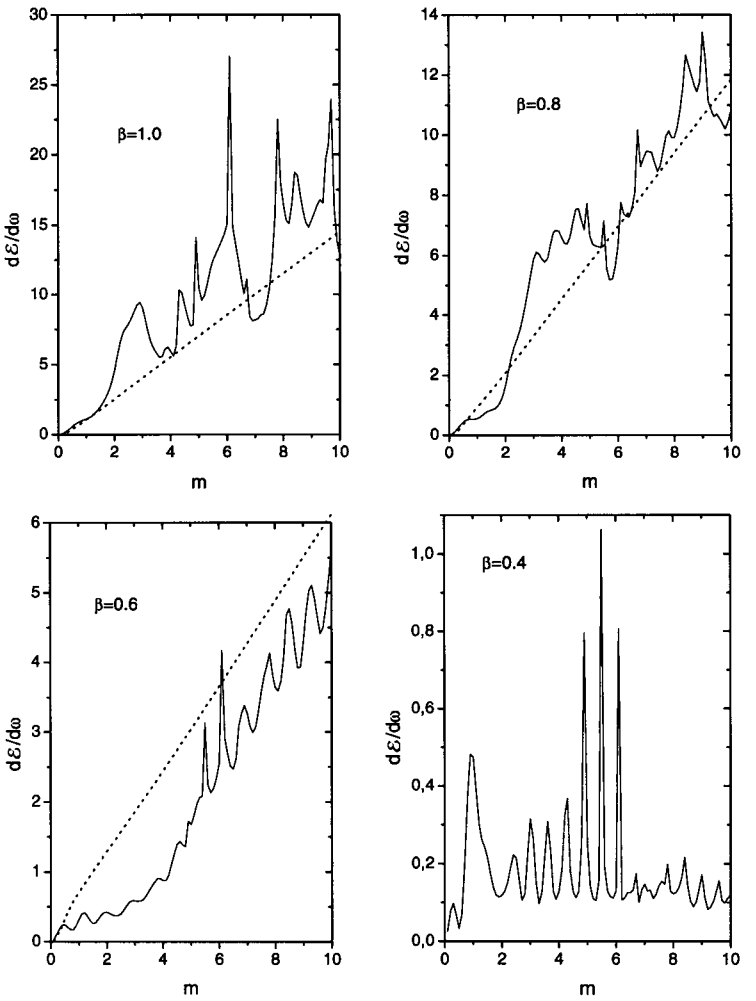

Figure 8: Frequency radiation intensities in e^2/c units (solid curves) for the charge motion shown in FIG. 6 and various charge velocities. The media parameters are the same as in FIG. 7. Further, $ka = m, kz_0 = 2m$. The dotted curves are the Tamm frequency intensities (3.5) evaluated for $kL = 2ka$ and $n = n_1$.

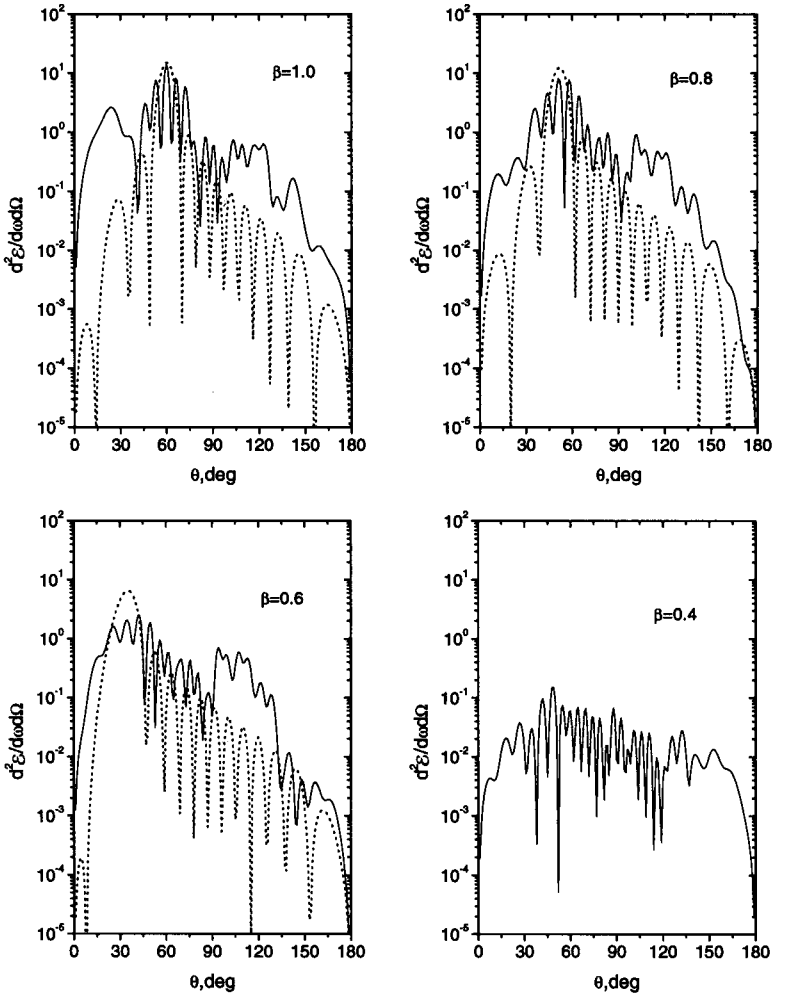

Figure 9: The same as in Fig. 7 but for $n_1 = 1, n_2 = 2$ (that is, there is vacuum inside S). The dotted curves are the Tamm angular intensities (3.4) evaluated for $kL = 2k(z_0 - a)$ and $n = n_2$.

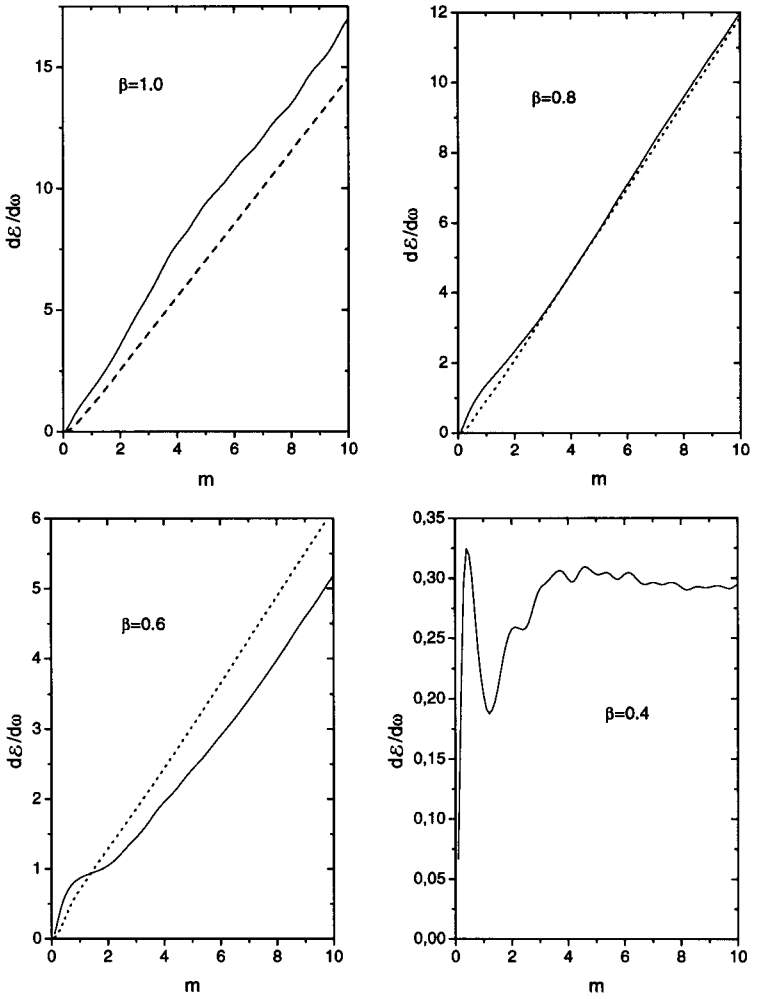

Figure 10: The same as in Fig. 8 but for $n_1 = 1, n_2 = 2$ (there is vacuum inside S). The dotted curves are the Tamm frequency intensities (3.5) evaluated for $kL = 2k(z_0 - a)$ and $n = n_2$.

$n = n_2, L = 2(z_0 - a)$ are shown. In the treated case, the part of the charge trajectory where $\beta n > 1$ lies outside the sphere S. We observe a satisfactory agreement of the exact intensity (5.8) with the Tamm intensity (3.4). Experimentalist studying, e.g., the electron passing through the dielectric sphere S, will see the pronounced Cherenkov maximum at $\theta = \theta_c$ ($\cos\theta_c = 1/\beta n$). The corresponding frequency distribution (5.3) does not differ appreciably from the Tamm one (3.5) (FIG. 10).

5.2 Metallic sphere

On the surface of ideal metal, tangential components of the electric field strength vanish [16]. For the metallic sphere of the radius a, this leads to the disappearance of E_θ. This defines $\tilde{C}_l$:

$$\tilde{C}_l = \tilde{J}_l^{(2)}(a, z_0) - \frac{J_l(2)}{H_l(2)}\tilde{H}_l^{(2)}(a, z_0) = \frac{i}{H_l(2)}[N_l(2)\tilde{J}_l^{(2)}(a, z_0) - J_l(2)\tilde{N}_l^{(2)}(a, z_0)]. \quad (5.10)$$

Then, angular and frequency distributions are given by (5.8),(5.9) but with $\tilde{C}_l$ defined by (5.10).

5.2.1 Numerical results

Let outside S be vacuum. The corresponding angular distributions (5.8) (solid lines) are compared in FIG. 11 with the Tamm angular intensities (3.4) (dotted lines) evaluated for $L = 2(z_0 - a)$ and $n = n_2$. Since $\beta n \leq 1$ outside the sphere S , the angular intensities are rather small.
The corresponding frequency distributions (5.9) (solid lines) and the Tamm ones (3.5) (dotted lines) are shown in FIG. 12. Their agreement is rather poor.

Let outside S be the medium with the refractive index $n_2 = 2$. The corresponding angular and frequency distributions are shown in FIGs. 13 and 14, resp. We observe the satisfactory agreement with the Tamm intensities evaluated for $L = 2(z_0 - a)$ and $n = n_2$.

6 Discussion

Formulae obtained in previous two sections describe the VC radiation, the radiation arising from the charge instantaneous acceleration and deceleration and the transition radiation arising from a charge passing from one medium to another.
To separate contribution of the transition radiation, one should subtract (according, e.g., to [5] or [17]) the field strengths corresponding to the inhomogenuous solution of the Maxwell equations from the total field strengths. In the treated case, the field strengths corresponding to the Tamm problem should be subtracted (they are written out in section III B). This leads to the following redefinition of the $\tilde{C}_l$ coefficients:

$$\tilde{C}_l \to \tilde{C}_l - \sqrt{\frac{n_1\mu_1}{n_2\mu_2}}\tilde{J}_l^{(1)}(0, z_0)$$

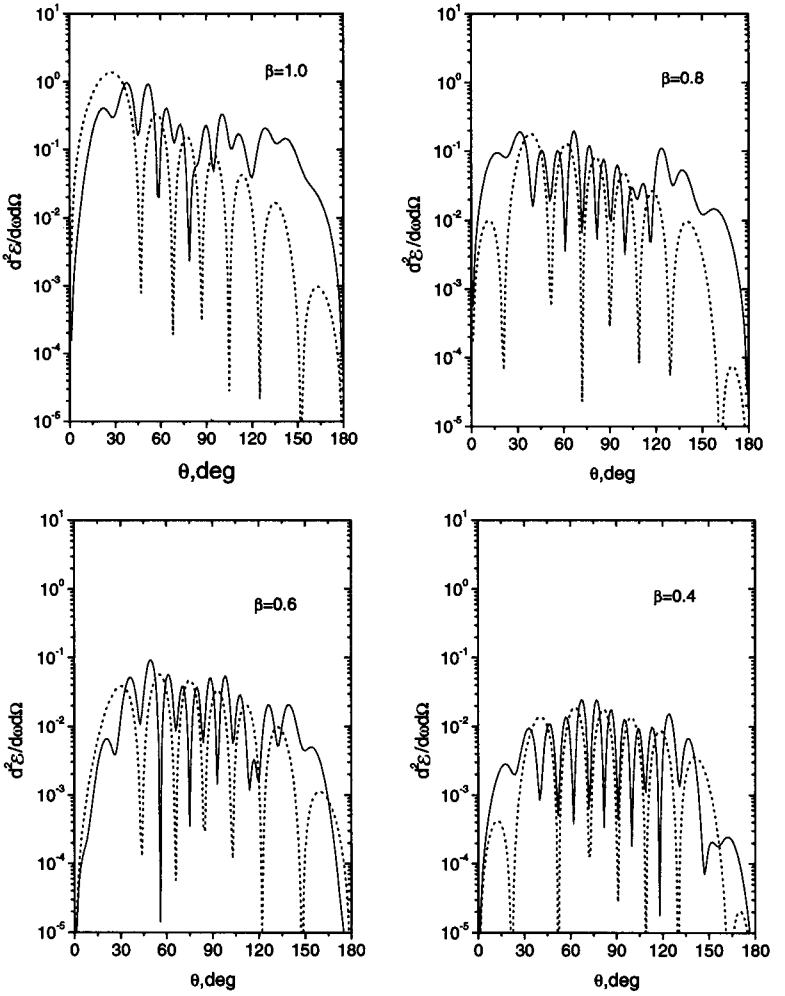

Figure 11: Angular radiation intensities in e^2/c units (solid curves) for the charge motion shown in FIG. 6 and various charge velocities. The medium inside S is ideal metallic substance. The medium refractive index outside S is $n_2 = 1$ (vacuum). Further, $ka = 10, kz_0 = 20$. The dotted curves are the Tamm angular intensities (3.4) evaluated for $kL = 2k(z_0 - a)$ and $n = n_2$.

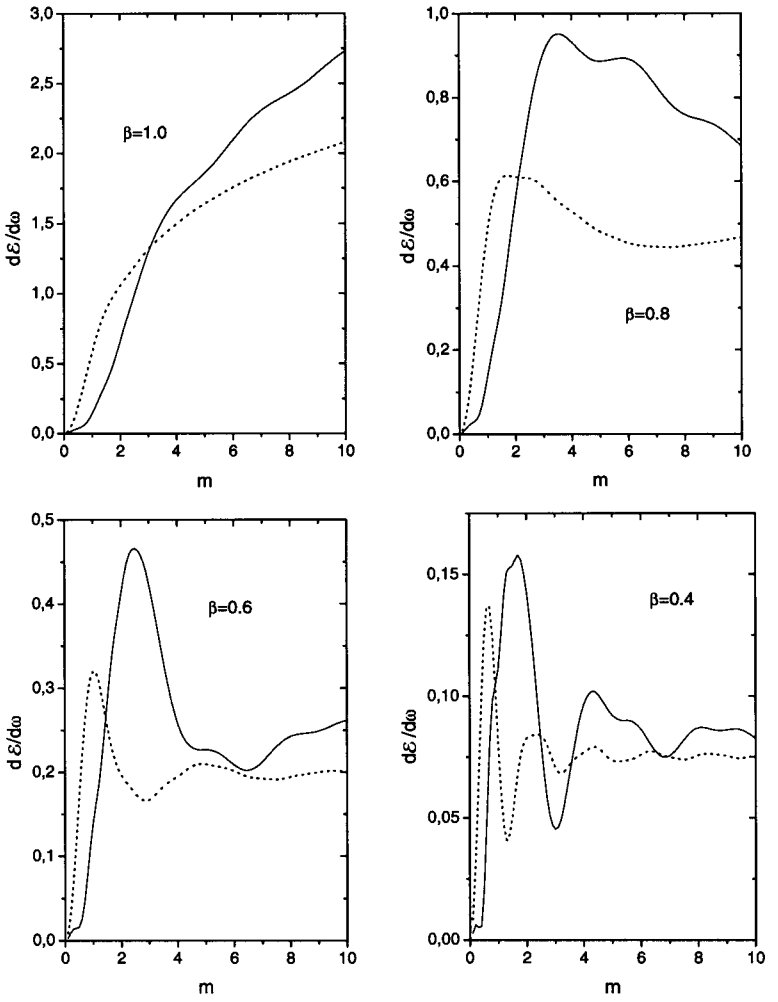

Figure 12: Frequency radiation intensities in e^2/c units (solid curves) for the charge motion shown in FIG. 6 and various charge velocities. The medium inside S is ideal metallic substance. The medium refractive index outside S is $n_2 = 1$ (vacuum). Further, $ka = m, kz_0 = 2m$. The dotted curves are the Tamm frequency intensities (3.5) evaluated for $kL = 2k(z_0 - a)$ and $n = n_2$.

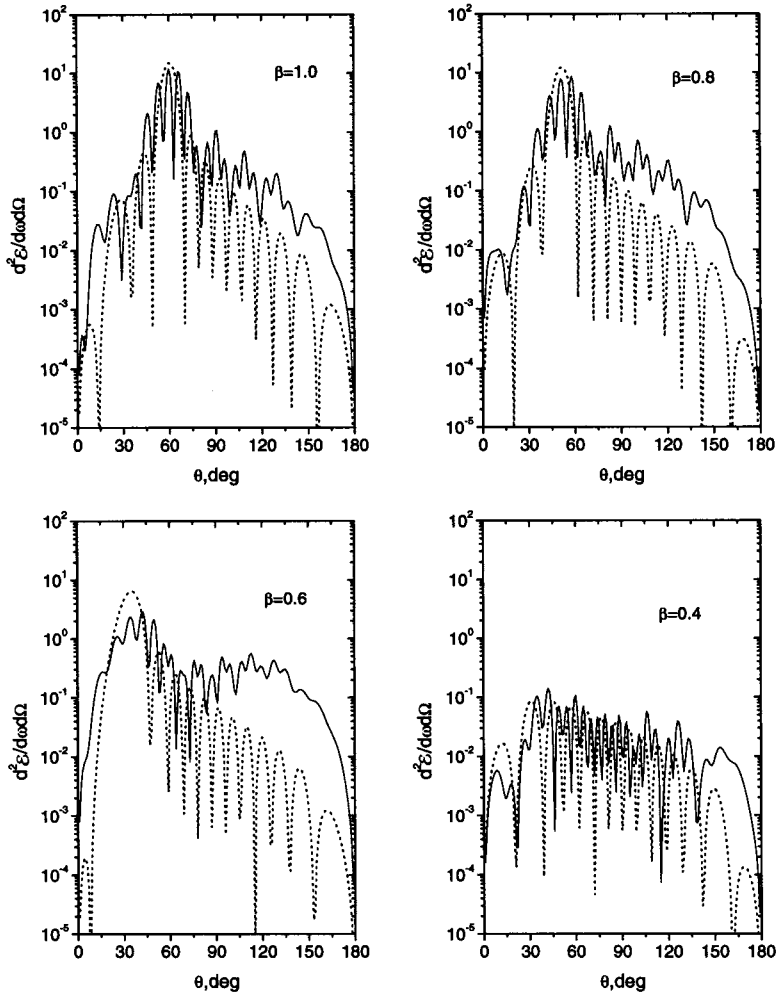

Figure 13: The same as in Fig. 11 but for metallic substance. The medium refractive index outside S is $n_2 = 2$. The dotted curves are the Tamm angular intensities (3.4) evaluated for $kL = 2k(z_0 - a)$ and $n = n_2$.

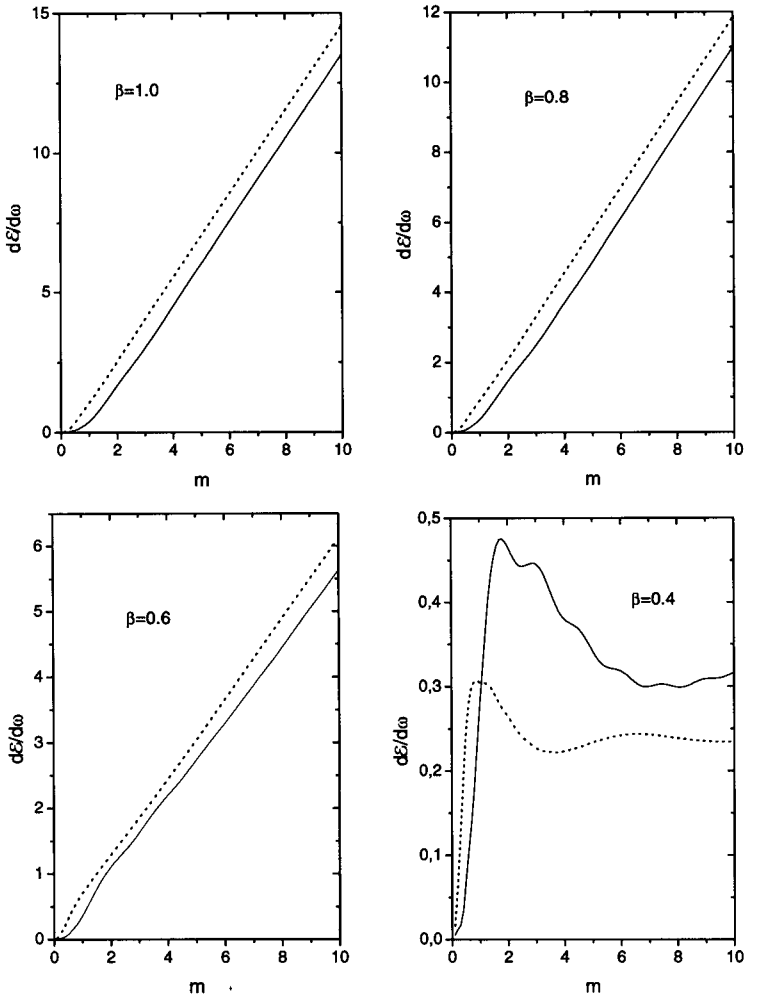

Figure 14: The same as in Fig. 12 but for $n_2 = 2$. The dotted curves are the Tamm frequency intensities (3.5) evaluated for $kL = 2k(z_0 - a)$ and $n = n_2$.

for the motion shown in Fig.1,

$$\tilde{C}_l \to \tilde{C}_l - \sqrt{\frac{n_1\mu_1}{n_2\mu_2}}\tilde{J}_l^{(1)}(0,a) - J_l^{(2)}(a,z_0)$$

for the charge motion through the dielectric sphere (Fig. 7) and

$$\tilde{C}_l \to \tilde{C}_l - J_l^{(2)}(a,z_0)$$

for the charge motion through the metallic sphere (Fig. 7). These newly defined $\tilde{C}_l$ being substituted into (4.7), (4.8), (5.8) and (5.9) give transition radition intensities. Due to the lack of space and since the observable radiation intensities are the total ones presented in Figs. 2-5 and 7-14, we do not evaluate transition radiation intensities in this paper.

In the physical literature there are semi-intuitive interpretations of the transition radiation and the one arising in the Tamm problem in terms of instantaneous acceleration and deceleration, and in terms of semi-infinite charge motion terminating at one side of the media interface and beginning at the other one. Their insufficiencies (discussed below) prevent us from their applying to the consideration of VC and transition radiation on the spherical sample. In any case, exact solutions and numerical calculations presented in sections IV and V contain all necessary information for the analysis of experimental data.

6.1 Comment on the transition radiation

6.1.1 Interpretation of the transition radiation in terms of instantaneous velocity jumps

Sometimes the transition radiation is interpreted as a charge uniform motion with the velocity v in medium 1, its sudden stop in medium 1 at the border with medium 2, the sudden start of motion in medium 2 and the charge uniform motion in medium 2 with the velocity v (see, e.g., [18–20]). It is suggested that the main contribution to the radiation intensity give the mentioned above instantaneous jumps of the charge velocity. The radiation intensity arising from the charge sudden stop in medium 1 is taken in the form

$$\frac{d^2\mathcal{E}}{d\omega d\Omega} = \frac{e^2}{4\pi^2 c}\left[\frac{\vec{\beta}\times\vec{n}_r}{1-n_1(\vec{\beta}\vec{n}_r)}\right]^2, \tag{6.1}$$

where $\vec{\beta} = \vec{v}/c$, $\vec{n}_r$ is the unit radius vector of the observation point and n_1 is the refractive index of the medium 1.

On the other hand, the exact calculations were made in [21] for the following decelerated motion along the z axis:

$$z(t) = z_1 + v_1(t-t_1) - \frac{1}{2}a(t-t_1)^2, \quad v(t) = v_1 - a(t-t_1), \quad t_1 < t < t_2 \tag{6.2}$$

which begins at the moment t_1 at the space point z_1 with the velocity v_1 and ends at the moment t_2 at the space point z_2 with the velocity v_2. The time motion interval $t_2 - t_1$ and deceleration a are easily expressed through z_1, z_2, v_1 and v_2

$$t_2 - t_1 = 2\frac{z_2 - z_1}{v_1 + v_2}, \quad a = \frac{1}{2}\frac{v_1^2 - v_2^2}{z_2 - z_1}. \tag{6.2'}$$

It was shown in [21] that for the fixed wavelength λ, the intensity of radiation tends to zero for $k(z_2 - z_1) \to 0$ ($k = 2\pi/\lambda$). This certainly disagrees with (6.1) which differs from zero for any motion interval. To clarify the situation, we turn to the derivation of (6.1).

6.1.2 The derivation of (6.1)

For simplicity, we consider at first a charge motion in vacuum closely following Landau and Lifshitz treatise [22]. Its authors begin with the equations

$$\vec{H} = (\vec{n}_r \times \vec{E}), \quad \vec{E} = -\frac{1}{c}\dot{\vec{A}}$$

which are valid in the wave zone (the dot above the vector potential $\vec{A}$ means the differentiation over the laboratory time). For the Fourier transform of $\vec{H}$ one gets

$$\vec{H}_\omega = -\frac{1}{2\pi c}\int_{-\infty}^{\infty}(\vec{n}_r \times \dot{\vec{A}})\exp(i\omega t)dt. \tag{6.3}$$

Now, if $\vec{A} \neq 0$ for $t_1 < t < t_2$, then for $\omega(t_2 - t_1) << 1$ one can put $\exp(i\omega t) \approx 1$, thus obtaining

$$\vec{H}_\omega = -\frac{1}{2\pi c}\int \vec{n}_r \times \frac{\partial \vec{A}}{\partial t}dt = -\frac{1}{2\pi c}\vec{n}_r \times (\vec{A}_2 - \vec{A}_1). \tag{6.4}$$

Here $\vec{A}_2 = \vec{A}(t = t_2)$ and $\vec{A}_1 = \vec{A}(t = t_1)$. Further, authors of [22] change $\vec{A}_1$ and $\vec{A}_2$ by the Lienard-Wiechert potentials. This gives

$$\vec{H}_\omega = \frac{e}{2\pi cr}[\frac{\beta_2 \times n_r}{1 - (\vec{\beta}_2\vec{n}_r)} - \frac{\beta_1 \times n_r}{1 - (\vec{\beta}_1\vec{n}_r)}]. \tag{6.5}$$

The radiation intensity per unit frequency and per unit solid angle is

$$\frac{d^2\mathcal{E}}{d\omega d\Omega} = cr^2|\vec{H}_\omega|^2 = \frac{e^2}{4\pi^2 c}[\frac{\beta_2 \times n_r}{1 - (\vec{\beta}_2\vec{n}_r)} - \frac{\beta_1 \times n_r}{1 - (\vec{\beta}_1\vec{n}_r)}]^2. \tag{6.6}$$

Now if the final velocity is zero, (6.6) coincides with (6.1).

6.1.3 Resolution of paradox

We rewrite the integral entering into (6.4) in the form

$$\int \frac{\partial \vec{A}}{\partial t}dt = \int \frac{\partial \vec{A}(t(t'))}{\partial t'}dt' = \vec{A}_2 - \vec{A}_1, \tag{6.6}$$

where t' is the charge retarded (proper) time. The laboratory times t_1 and t_2 being expressed through the retarded times for the one dimensional motion along the z axis are given by

$$t_1 = t_1' + \frac{1}{c}[\rho^2 + (z - z_1')^2]^{1/2}, \quad t_2 = t_2' + \frac{1}{c}[\rho^2 + (z - z_2')^2]^{1/2}, \tag{6.7}$$

where $z'_1 = z'(t'_1)$ and $z'_2 = z'(t'_2)$ are the charge positions at the times t'_1 and t'_2. Now, let the charge proper time t' be uniquely related to its position z'. Then, for $z'_1 = z'_2$, one gets $t'_1 = t'_2$, $t_1 = t_2$ and, therefore, $\vec{A}_2 = \vec{A}_1$, $\vec{H}_\omega = 0$ and $d^2\mathcal{E}/d\omega d\Omega = 0$.
We illustrate this using the motion law (6.2) as an example (note that t and z entering into (6.2) are the charge proper time t' and its position z'). For this motion law, t' is uniquely related to z':

$$t' = t_1 + 2v_1\frac{z_2 - z_1}{v_1^2 - v_2^2}[1 - (1 - \frac{z' - z_1}{z_2 - z_1}\frac{v_1^2 - v_2^2}{v_1^2})^{1/2}]. \tag{6.8}$$

According to (6.2'), $t_2 = t_1$ for $z_2 = z_1$. Therefore, $\vec{A}_2 = \vec{A}_1$ for $t_2 = t_1$ and $\vec{H}_\omega$ given by (6.4) vanishes in the $k(z_2 - z_1) \to 0$ limit, in accordance with [21].

The main assumptions for the vanishing of $\vec{H}_\omega$ are: i) the discontinuous charge motion with the velocity jumps can be viewed as a limiting case of the continuous motion without the velocity jumps when the length along which the velocity changes from v_1 to v_2 tends to zero; ii) the retarded (proper) charge time is uniquely related to its position.

We conclude: the interpretation of the transition radiation in terms of the charge instantaneous acceleration and deceleration at the border of two media is not sufficient if the discontinuous charge motion can be treated as a limiting case of the continuous charge motion. In any case, the discontinuous charge motion cannot be realized in nature: it is the suitable idealization of some continuous charge motion.

In general, $\vec{A}(t_2)$ does not coincide with $\vec{A}(t_1)$ if the charge proper time is not uniquely related to its position. Consider, for example, the immovable elementary (infinitesimal) time dependent source. Then, $\vec{A}(t_2) \neq \vec{A}(t_1)$ and $\vec{H}_\omega \neq 0$. Another possibility to obtain $\vec{A}(t_2) \neq \vec{A}(t_1)$ is to take into account the internal degrees of freedom of a moving charged particle (for example, its spin flip at the fixed space point can give $\vec{A}(t_2) \neq \vec{A}(t_1)$).

6.1.4 On the interpretation of the transition radiation in terms of the charge semi-infinite motions

In Refs. [4,5], the transition radiation was associated with the charge radiation on the semi-infinite intervals $(-\infty, 0)$ and $(0, \infty)$ lying in media 1 and 2, resp. We analyse this situation using the vector potential as an example. VP corresponding to the charge motion in medium 1 is given by

$$A_z = \frac{e\mu_1}{2\pi c}\int\limits_{-\infty}^{0}\frac{dz'}{R}\exp(i\psi), \tag{6.9}$$

where $\psi = kz'/\beta + k_1 R$, $\quad k_1 = kn_1$, $\quad R = \sqrt{\rho^2 + (z - z')^2}$. In the quasiclassical approximation one gets

$$A_z^{(1)} = \frac{e\mu_1}{2\pi cr}\frac{1}{1 - \beta_1\cos\theta} \tag{6.10}$$

for $\beta < \beta_1 = 1/n_1$. For $\beta > \beta_1$,

$$A_z^{(1)} = (6.10) \quad \text{for} \quad \theta < \theta_1 \quad \text{and}$$

$$A_z^{(1)} = (6.10) + A_T^{(1)} \quad \text{for} \quad \theta > \theta_1.$$

Here

$$A_T^{(1)} = \frac{e\mu_1}{2\pi c}\exp(\frac{i\pi}{4})\sqrt{\frac{2\pi\beta\gamma_1}{kr\sin\theta}}\exp[\frac{ikr}{\beta}(\cos\theta + \frac{\sin\theta}{\gamma_1})], \quad \gamma_1 = \frac{1}{\sqrt{|1-\beta_1^2|}}, \quad \cos\theta_1 = \frac{1}{\beta_1}. \tag{6.11}$$

Since $A_T(1)$ decreases like $1/\sqrt{kr}$, the radiation intensity is large in the $\theta > \theta_1$ angular region.

Similarly, the vector potential corresponding to the charge motion in medium 2 is given by

$$A_z^{(2)} = -\frac{e\mu_2}{2\pi cr}\frac{1}{1-\beta_2\cos\theta} \quad \text{for} \quad \beta < \beta_2 = 1/n_2. \tag{6.12}$$

For $\beta > \beta_2$,

$$A_z^{(2)} = (6.12) \quad \text{for} \quad \theta > \theta_2 \quad \text{and}$$
$$A_z^{(2)} = (6.12) + A_T^{(2)} \quad \text{for} \quad \theta < \theta_2.$$

Here

$$A_T^{(2)} = \frac{e\mu_2}{2\pi c}\exp(\frac{i\pi}{4})\sqrt{\frac{2\pi\beta\gamma_2}{kr\sin\theta}}\exp[\frac{ikr}{\beta}(\cos\theta + \frac{\sin\theta}{\gamma_2})], \quad \gamma_2 = \frac{1}{\sqrt{|1-\beta_2^2|}}, \quad \cos\theta_2 = \frac{1}{\beta_2}. \tag{6.13}$$

Usually, the terms $A_T^{(1)}$ and $A_T^{(2)}$ are dropped in standard considerations of the transition radiation. Their interference with $A_z^{(1)}$ and $A_z^{(2)}$ given by (6.11) and (6.12), resp., leads to the oscillations of the radiation intensity in the $\theta > \theta_1$ angular region for the charge semi-infinite motion $(-\infty, 0)$ in medium 1, and in the $\theta < \theta_2$ angular region for the charge semi-infinite motion $(0, \infty)$ in medium 2.

A further procedure in obtaining the transition radiation intensities is the evaluation of EMF strengths corresponding to vector potentials in media 1 and 2 and their superposition with corresponding Fresnel coefficients . Sometimes the secondary photon rescatterings at the boundaries of media 1 and 2 (for the dielectric plate) are taken into account.

Since we have at hand the exact solution for the charge moving inside and outside the dielectric or metallic sphere, these tricks are not needed: they are automatically taken into account in closed expressions for radiation intensities.

6.1.5 On the physical meaning of $A_T^{(1)}$ and $A_T^{(2)}$ terms

To clarify the physical meaning of $A_T^{(1)}$ and $A_T^{(2)}$ terms, we consider the case when media 1 and 2 are the same. Then, the vector potential corresponding to the infinite motion $(-\infty, \infty)$ reduces to the sum of vector potentials corresponding to semi-infinite motions in media 1 and 2:

$$A_z = A_z^{(1)} + A_z^{(2)} = 0$$

for $\beta < 1/n$ and

$$A_z = A_T^{(1)} + A_T^{(2)} = \frac{e\mu}{2\pi c}\exp(\frac{i\pi}{4})\sqrt{\frac{2\pi\beta\gamma_n}{kr\sin\theta}}\exp[\frac{ikr}{\beta}(\cos\theta + \frac{\sin\theta}{\gamma_n})], \quad \gamma_n = \frac{1}{\sqrt{|1-\beta_n^2|}} \tag{6.14}$$

for $\beta > 1/n$. But this is the asymptotic form ($\rho \to \infty$) of the VC vector potential corresponding to the charge infinite motion in unbounded medium

$$A_z = \frac{e\mu}{\pi c} K_0(\frac{k\rho}{\beta\gamma_n}) \quad \text{for} \quad \beta < \frac{1}{n} \quad \text{and} \quad A_z = \frac{ie\mu}{2c} \exp(\frac{ikz}{\beta}) H_0^{(1)}(\frac{k\rho}{\beta\gamma_n}) \quad \text{for} \quad \beta > \frac{1}{n}.$$

This means that $A_T^{(1)}$ and $A_T^{(2)}$ terms describe the VC radiation for the semi-infinite charge motions in media 1 and 2. This is also confirmed by the exact solution corresponding to the semi-infinite charge motion in dispersion free medium found in [23,24] in the time representation. Indeed, the space regions where the VC radiation differs from zero are just the same where $A_T^{(1)}$ and $A_T^{(2)}$ terms differ from zero.

It is easy to check that the values of $A_z^{(1)}$ and $A_z^{(2)}$ are defined by the boundary point $z' = 0$, while the values of $A_T^{(1)}$ and $A_T^{(2)}$ terms are defined by stationary points z' lying in the intervals $(-\infty, 0)$ and $(0, \infty)$, resp.

We see that the interpretation of the transition radiation in terms of semi-infinite motions in the intervals $(-\infty, 0)$ and $(0, \infty)$ is sufficient only for $\beta < 1/n$. On the other hand, for $\beta > 1/n$, the Cherenkov terms $A_T^{(1)}$ and $A_T^{(2)}$ should be taken into account.

6.2 Comment on the Tamm problem

For the Tamm problem (uniform charge motion in a restricted space interval), the vector potential is given by (3.1). It is easily evaluated in the quasiclassical approximation. For $z < \rho\gamma_n - z_0$ and $z > \rho\gamma_n + z_0$ one gets

$$A_z^{out} = -\frac{ie\mu\beta}{2\pi ck}\{\frac{1}{r_2 - \beta_n(z - z_0)} \exp[\frac{ik}{\beta}(\beta n r_2 + z_0)] -$$

$$-\frac{1}{r_1 - \beta_n(z + z_0)} \exp[\frac{ik}{\beta}(\beta n r_1 - z_0)]\}. \tag{6.15}$$

Here $r_1 = \sqrt{\rho^2 + (z + z_0)^2}$ and $r_2 = \sqrt{\rho^2 + (z - z_0)^2}$. Inside the interval $\rho\gamma_n - z_0 < z < \rho\gamma_n + z_0$, the vector potential equals

$$A_z^{in} = A_z^{out} + A_z^{Ch}, \tag{6.16}$$

where

$$A_z^{Ch} = \frac{e\mu}{2\pi c} \exp(\frac{ikz}{\beta}) \sqrt{\frac{2\pi\beta\gamma_n}{kr\sin\theta}} \exp(i\frac{\pi}{4}) \exp(\frac{ikr\sin\theta}{\beta\gamma_n}).$$

It is seen that A_z^{out} is infinite at $z = \rho\gamma_n \pm z_0$ (this is due to the quasiclassical approximation used). Therefore, the radiation intensity should have maxima at $z = \rho\gamma_n \pm z_0$, with a kind of plato for $\rho\gamma_n - z_0 < z < \rho\gamma_n + z_0$ and a sharp decreasing for $z < \rho\gamma_n - z_0$ and $z > \rho\gamma_n + z_0$. At the observation distances much larger than the motion length

$$r_1 - \beta_n(z + z_0) \approx r(1 - \beta_n\cos\theta), \quad r_2 - \beta_n(z - z_0) \approx r(1 - \beta_n\cos\theta),$$

$$\beta_n r_1 - z_0 = \beta_n r - z_0(1 - \beta_n\cos\theta), \quad \beta_n r_2 + z_0 = \beta_n r + z_0(1 - \beta_n\cos\theta).$$

Then,

$$A_z^{out} = \frac{e\mu\beta}{\pi ckr} \exp(iknr) \frac{\sin[\omega t_0(1 - \beta n\cos\theta)]}{1 - \beta n\cos\theta}, \tag{6.17}$$

that coincides with the Tamm vector potential A_z^T entering into (3.2). Thus, inside the interval $\rho\gamma_n - z_0 < z < \rho\gamma_n + z_0$,

$$A_z^{in} = A_z^T + A_z^{Ch}. \tag{6.18}$$

We observe that infinities of A_z^{out} disappeared due to the approximations involved. It is seen that for $kr >> 1$, A_z^{Ch} and A_z^T behave like $1/\sqrt{kr}$ and $1/kr$, resp. It follows from this that the radiation intensity in space regions $z > \rho\gamma_n + z_0$ and $z < \rho\gamma_n - z_0$ is described by the Tamm formula (3.4). On the other hand, inside the space region $\rho\gamma_n - z_0 < z < \rho\gamma_n + z_0$, the radiation intensity differs appreciably from the Tamm one. In fact, the second term in A_z^{in} is much larger than the first one (A_z^T) for $kr >> 1$ (since they decrease like $1/\sqrt{kr}$ and $1/kr$ for $kr \to \infty$, resp.) It is easy to check that on the surface of the sphere of the radius r, the intervals $z < \rho\gamma_n - z_0$, $\rho\gamma_n - z_0 < z < \rho\gamma_n + z_0$ and $z > \rho\gamma_n + z_0$ correspond to angular intervals $\theta > \theta_1$, $\theta_2 < \theta < \theta_1$ and $\theta < \theta_2$, where θ_1 and θ_2 are defined by

$$\cos\theta_1 = -\frac{\epsilon_0}{\beta_n^2\gamma_n^2} + \frac{1}{\beta_n}[1 - (\frac{\epsilon_0}{\beta_n\gamma_n})^2]^{1/2}$$

and

$$\cos\theta_2 = \frac{\epsilon_0}{\beta_n^2\gamma_n^2} + \frac{1}{\beta_n}[1 - (\frac{\epsilon_0}{\beta_n\gamma_n})^2]^{1/2}. \tag{6.19}$$

Here $\epsilon_0 = z_0/r$. For $r >> z_0$,

$$\theta_1 = \theta_c + \frac{\epsilon_0}{\beta_n\gamma_n}, \quad \theta_2 = \theta_c - \frac{\epsilon_0}{\beta_n\gamma_n},$$

where θ_c is defined by $\cos\theta_c = 1/\beta n$. Therefore, inside the angular interval $\theta_2 < \theta < \theta_1$ the radiation intensity should have plato with its height proportional to the observation distance r. In the limit $r \to \infty$, the above θ interval diminishes and for the radiation intensity one gets the δ- type singularity at $\cos\theta = 1/\beta n$ (in addition to A_z^T). However, the θ integral from it is finite. Although $\Delta\theta = \theta_1 - \theta_2 = 2\epsilon_0/\beta_n\gamma_n$ is very small for $r >> z - 0$, the length of arc on the observation sphere on which the radiation intensity differs from the Tamm one is finite: it is given by $2z_0/\beta_n\gamma_n$. It would be interesting to observe this deviation experimentally (there are recent experimental indications for the existence of this plato [25]).

From the previous consideration it follows that A_z^{Ch} is a part of the Cherenkov shock wave enclosed between straight lines $z = -z_0 + \rho\gamma_n$ and $z = z_0 + \rho\gamma_n$ inclined under the angle θ_c towards the motion axis. In the quasiclassical approximation, the stationary point $z' = z - \rho\gamma_n$ of the integral α_T entering in (3.1) lies inside the motion interval $(-z_0, z_0)$ and defines the value of A_z^{Ch}. On the other hand, for the A_z^{out} the stationary point of α_T lies outside the charge motion interval and the value of α_T is defined by initial and final points of the motion interval. Therefore, A_z^{out} is somehow related to the beginning and the end of motion. In [26,27] the radiation intensity in the Tamm problem was associated with the interference of bremsstrahlung shock waves arising from the instantaneous velocity jumps at the beginning and the end of motion. However, if one replaces the instantaneous velocity jumps by the smoothed ones and then tends the width of the transition region (where the velocity smoothly changes) to zero then the

contribution of this region to the radiation intensity also tends to zero [21]. There are no velocity jumps for this smoothed motion and, therefore, the radiation intensity in the Tamm problem cannot be attributed to them. However, there are acceleration jumps at the beginning and the end of motion and at the moments when the accelerated motion meets the uniform one. Thus, the above intensity can be still associated with acceleration jumps. To clarify the situation, the Tamm problem with absolutely continuous charge motion (for which the velocity itself and all its time derivatives are absolutely continuous functions of time) was considered in [28]. It was shown that the relatively slow decreasing of the radiation intensity outside the plato is replaced by its exponential damping. This means that the discontinuities of higher derivatives of the charge velocity contribute to the asymptotic behaviour of the radiation intensities as well. Formerly, for the charge motion in vacuum, the exponential damping for all angles was recognized in [29–32]. We conclude: the instantaneous velocity jumps at the beginning and the end of motion do not contribute to the radiation intensity provided they can be viewed as the limiting cases of the smooth charge motion in the limit when the lengths of accelerated (decelerated) pieces of the charge trajectory tend to zero. This means that attempts to interpret the radiation intensity given by the Tamm formula (3.4) in terms of the charge instantaneous acceleration and deceleration are insufficient.

We summarize discussion:

1) the interpretation of the transition radiation and the Tamm problem in terms of instantaneous acceleration and deceleration is not sufficient;

2) the usual interpretation of the radiation arising when the charge crosses the boundary between two media in terms of semi-infinite charge motions is valid only if $\beta < 1/n_1$ and $\beta < 1/n_2$. Otherwise, this interpretation should be supplemented by the Cherenkov-like terms;

3) there is no need in artificial means mentioned in previous two items in the treated exactly solvable case corresponding to the transition and VC radiations on a spherical sample.

7 Conclusion

We briefly review the main results obtained:

1) The electromagnetic field strengths and angular radiation intensity corresponding to the Tamm problem are developed in terms of Legendre polynomials. The corresponding representation for the frequency distributions is also found.

2) We found closed expressions for the electromagnetic field arising from the charge motion confined to the dielectric sphere S which is surrounded by another dielectric medium with dielectric properties different from those inside S. It is studied how differences of media properties inside and outside S affect the angular and frequency radiation intensities for various charge velocities. In general, these differences lead to the broadening of the angular spectrum to the rise of angular intensities at large angles, and to the appearance of oscillations in the frequency spectrum.

3) It is considered how radiates a charge whose motion begins and terminates in medium 2 and which passes through the dielectric sphere S filled with medium 1 or through the metallic sphere. The evaluated energy flux includes the VC and transition radiations as well as ones originating from the beginning and termination of motion. It is shown that

when the medium 2 outside S is vacuum and medium 1 inside S has refractive index n_1 satisfying $\beta n_1 > 1$, the angular and frequency radiation intensities cannot be always interpreted in terms of the Tamm formula (3.4) corresponding to the charge motion inside S (as it is usually believed).
4) It is proved that the interpretation of the transition radiation in terms of the instantaneous termination of the charge motion in one medium and its instantaneous beginning in the other one is not valid if the above motion with sudden velocity jumps can be considered as a limiting case of the smooth charge motion. It is shown that the interpretation of the transition radiation in terms of semi-infinite motions with instantaneous termination of the charge motion in one medium and with its instantaneous beginning in the other one, should be supplemented with the VC radiation terms. Certainly, these remarks are related only to the interpretation of the transition radiation, not to the exact solutions obtained for the plane interface , e.g., in [5,17].

Acknowledgement

The authors are thankful to referee for his valuable comments.

Appendix 1

Using (2.3),(2.4) and (3.8) we find that the magnetic vector potential corresponding to Fig.1 equals

$$A_z = \frac{iek_2\mu_2}{2\pi c}\sum(2l+1)P_l(\cos\theta)h_l(k_2r)C_l$$

for $r > a$,

$$A_z = \frac{iek_1\mu_1}{2\pi c}\sum(2l+1)P_l(\cos\theta)[j_l(k_1r)D_l + h_l(k_1r)J_l^{(1)}(0,z_0)],$$

for $z_0 < r < a$ and

$$A_z = \frac{iek_1\mu_1}{2\pi c}\sum(2l+1)P_l(\cos\theta)[j_l(k_1r)D_l + h_l(k_1r)J_l^{(1)}(0,r) + j_l(k_1r)H_l^{(1)}(r,z_0)]$$

for $r < z_0$. Here we put

$$J_l^{(1)}(x,y) = \int_x^y j_l(k_1r')f_l(r')dr' \quad H_l^{(1)}(x,y) = \int_x^y h_l(k_1r')f_l(r')dr.'$$

Differentiating A_z, one finds EMF strengths (4.1),(4.2) in which

$$\tilde{C}_l = C_{l-1} + C_{l+1}, \quad \text{and} \quad \tilde{D}_l = D_{l-1} + D_{l+1}$$

Since EMF strengths contain only $\tilde{C}_l$ and $\tilde{D}_l$, the coefficients C_l and D_l entering into electromagnetic potentials are not needed.

Appendix 2

The magnetic vector potential satisfying equations $(\triangle + k_2^2)A_z = 0$ for $r > z_0$, $(\triangle + k_2^2)A_z = -4\pi\mu_2 j_z/c$ for $a < r < z_0$ and $(\triangle + k_1^2)A_z = -4\pi\mu_1 j_z/c$ for $r < a$ is given by

$$A_z = \frac{iek_2\mu_2}{2\pi c}\sum(2l+1)P_l h_l(k_2 r)[C_l\frac{\mu_1}{\mu_2}J_l^{(1)}(0,a) + J_l^{(2)}(a,z_0)],$$

for $r > z_0$,

$$A_z = \frac{iek_2\mu_2}{2\pi c}\sum(2l+1)P_l[h_l(k_2 r)C_l\frac{\mu_1}{\mu_2}J_l^{(1)}(0,a) + h_l(k_2 r)J_l^{(2)}(a,r) + j_l(k_2 r)H_l^{(2)}(r,z_0)]$$

for $a < r < z_0$ and

$$A_z = \frac{iek_1\mu_1}{2\pi c}\sum(2l+1)P_l(\cos\theta)\times$$

$$[j_l(k_1 r)\frac{\mu_2}{\mu_1}D_l H_l^{(2)}(a,z_0) + h_l(k_1 r)J_l^{(1)}(0,r) + j_l(k_1 r)H_l^{(1)}(r,a)]$$

for $r < a$. Here

$$J_l^{(2)}(x,y) = \int_x^y j_l(k_2 r')f_l(r')dr' \quad H_l^{(2)}(x,y) = \int_x^y h_l(k_2 r')f_l(r')dr.'$$

It is convenient to redefine C_l and D_l:

$$C_l' = C_l\frac{\mu_1}{\mu_2}J_l^{(1)}(0,a) + J_l^{(2)}(a,z_0), \quad D_l' = D_l\frac{\mu_2}{\mu_1}H_l^{(2)}(a,z_0).$$

Then,

$$A_z = \frac{iek_2\mu_2}{2\pi c}\sum(2l+1)P_l h_l(k_2 r)C_l'$$

for $r > z_0$,

$$A_z = \frac{iek_2\mu_2}{2\pi c}\sum(2l+1)P_l(\cos\theta)[C_l' h_l(k_2 r) - h_l(k_2 r)J_l^{(2)}(r,z_0) + j_l(k_2 r)H_l^{(2)}(r,z_0)]$$

for $a < r < z_0$ and

$$A_z = \frac{iek_1\mu_1}{2\pi c}\sum(2l+1)P_l(\cos\theta)[D_l' j_l(k_1 r) + h_l(k_1 r)J_l^{(1)}(0,r) + j_l(k_1 r)H_l^{(1)}(r,a)].$$

for $r < a$. Differentiating A_z, one recovers EMF strengths (5.1)-(5.3) where

$$\tilde{C}_l = C_{l-1}' + C_{l+1}', \quad \tilde{D}_l = D_{l-1}' + D_{l+1}'.$$

Again, we do not need coefficients C_l and D_l entering into the vector potential since EMF field strengths (and the radiation intensity) depend only on $\tilde{C}_l$ and $\tilde{D}_l$.

References

[1]P.A. Cherenkov, Trudy FIAN, **2**, No 4, 3(1944).

[2]V.L. Ginzburg and I.M. Frank, Dokl. Acad. Nauk SSSR, **56**, 609 (1947).

[3]G.N. Afanasiev, V.M. Shilov and Yu.P. Stepanovsky, J. Phys. D, **36**, 88 (2003).

[4]V.L. Ginzburg and I.M. Frank, JETP, **16**, 15 (1946).

[5]V.L. Ginzburg and V.N. Tsytovich, *Transition radiation and transition scattering*, (Moscow, Nauka,1984).

[6]I.S. Gradshteyn and I.M. Ryzik, *Tables of Integrals, Series and Products*, (New York, Academic Press, 1965).

[7]I.E. Tamm, J.Phys. USSR, **1**, 439 (1939).

[8]A.P. Kobzev and I.M. Frank, Sov. J. Nucl.Phys., **34**, 71 (1981).

[9]G.N. Afanasiev, V.G. Kartavenko and J. Ruzicka, J. Phys. A, **33**, 7585 (2000).

[10]I.M. Frank, *Vavilov-Cherenkov Radiation*, (Moscow, Nauka, 1988).

[11] D.K. Aitken, R.E. Jennings, A.S.L. Parsons and R.N.F. Walker, Proc. Phys. Soc., **82**, 710 (1963).

[12] A.P. Kobzev, A. Krawczyk and J. Rutkowski, Acta Physica Polonica, **B19**, 853 (1988).

[13] A. Bodek et al., Z.Phys., **C 18**, 289 (1983).

[14] M.G. Bowler, Nucl. Instr. Meth., **A 378**, 463 (1996).

[15] V.P. Zrelov, M.Klimanova, V.P. Lupiltsev and J. Ruzicka, Nuclear Instr. Meth., **215**, 141 (1983).

[16]L.D. Landau and E.M. Lifshitz, *Electrodynamics of Continuous Media*, (Oxford, Pergamon, 1960).

[17]M.A. Tehr-Mikaelan, *The influence of medium on high-energy electromagnetic processes*, (Yerevan, Izdat. Akad. Nauk Arm. SSSR, 1969).

[18]L. Wartski, S. Roland, J. Lasalle, M. Bolore and G. Filippi, J. Appl. Phys., **46**, 3644 (1975).

[19]J. Ruzicka and V.P. Zrelov, Czech. J. Phys., **43**, 551 (1993).

[20]A. Hrmo and J. Ruzicka, Nucl. Instr. Meth. A **451**, 506 (2000).

[21]G.N. Afanasiev and V.M. Shilov, J. Phys. D, **35**, 854 (2002).

[22]L.D. Landau and E.M. Lifshitz, *The Classical Theory of Fields* (New York, Pergamon, 1962).

[23]G.N. Afanasiev, Kh. Beshtoev and Yu. Stepanovsky, Helv. Phys. Acta, **69**, 111 (1996).

[24]G.N. Afanasiev, V.G. Kartavenko and Yu.P. Stepanovsky, J. Phys. D, **32**, 2029 (1999).

[25]G.N. Afanasiev, V.G. Kartavenko and V.P. Zrelov JINR Preprint **E2-2003-83**, (2003).

[26]V.P. Zrelov and J. Ruzicka, Czech. J. Phys. B**39**, 368 (1989).

[27]V.P. Zrelov and J. Ruzicka, Czech. J. Phys., **42**, 45 (1992).

[28]G.N. Afanasiev, V.M. Shilov and Yu.P. Stepanovsky, Nuovo Cim. B**117**, 815 (2002).

[29]I.I. Abbasov, Kratkije soobchenija po fizike FIAN, No **1** 31 (1982); English translation: Soviet Physics-Lebedev Institute Reports, No.**1**, 25 (1982).

[30]I.I. Abbasov, Kratkije soobchenija po fizike FIAN, No **8**, 33 (1985). English translation: Soviet Physics-Lebedev Institute Reports, No. **8**, 36 (1985).

[31]I.I. Abbasov, V.M. Bolotovskii and V.A. Davydov, Usp. Fiz. Nauk, **149**, 709 (1986). English translation: Sov. Phys. Usp., **29** 788 (1986).

[32]B.M. Bolotovskii and V.A. Davydov, Izv. Vuzov, Radiofizika, No. **1**, 31 (1981).

Received on May 23, 2003.

Афанасьев Г. Н., Картавенко В. Г., Степановский Ю. П. E2-2003-99
Излучение Вавилова–Черенкова и переходное излучение
на диэлектрической и металлической сферах

Получены замкнутые выражения для угловой и спектральной интенсивностей излучения, которое возникает при движении заряда внутри диэлектрической сферы S, при выполнении измерений вне S (это соответствует типичной экспериментальной ситуации, когда заряд движется в одной среде, а измерения осуществляются в другой). Показано, что различия в свойствах среды внутри и вне S существенно меняют угловые и спектральные распределения излучения. Также изучаются свойства излучения, возникающего при движении заряда, начинающегося и оканчивающегося в среде 2 и проходящего через диэлектрическую или металлическую сферы. Поток энергии в среде 2 состоит из черенковского и тормозного излучений и излучения, связанного с началом и окончанием движения. Вычисленные при различных скоростях заряда и свойствах среды внутри и вне S угловые и спектральные распределения излучения показывают, что стандартное определение скорости заряда по излучению на той части его траектории, где $\beta n > 1$, не всегда правильно. Показано, что недостаточной является интерпретация переходного излучения в терминах мгновенной остановки заряда в одной среде и мгновенного начала движения в другой. Попытки интерпретации переходного излучения в терминах полубесконечного движения, оканчивающегося в одной среде и начинающегося в другой, являются правильными, если при $\beta n > 1$ принять во внимание излучение Вавилова–Черенкова.

Работа выполнена в Лаборатории теоретической физики им. Н. Н. Боголюбова ОИЯИ.

Препринт Объединенного института ядерных исследований. Дубна, 2003

Afanasiev G. N., Kartavenko V. G., Stepanovsky Yu. P. E2-2003-99
Vavilov–Cherenkov and Transition Radiations
on the Dielectric and Metallic Spheres

Closed expressions are obtained for angular and frequency radiation intensities produced by a charge moving inside the dielectric sphere S, with observations made outside S (in fact, this is a typical experimental situation when a charge moves in one medium while measurements are made in the other one). It is shown that the difference in media properties inside and outside S drastically affects angular and frequency distributions. Also, a charge motion is considered which begins and terminates in medium 2 and which passes either through the dielectric sphere filled with medium 1 or through the metallic one. The energy flux in medium 2 involves the Vavilov–Cherenkov, transition radiation and the one arising from the charge instantaneous beginning and termination of motion. The evaluated angular and frequency distributions for various charge velocities and medium properties inside and outside S show that the standard identification of the charge velocity by its radiation on the part of the charge trajectory where $\beta n > 1$ is not always valid. We analyse also the frequently used interpretation of the transition radiation in terms of instantaneous charge deceleration in one medium and its sudden acceleration in another one, and find them as to be insufficient. On the other hand, attempts to interpret the transition radiation in terms of semi-infinite motions terminating in one medium and beginning in the other one turn out to be correct if one takes into account the terms corresponding to the Vavilov–Cherenkov radiation.

The investigation has been performed at the Bogoliubov Laboratory of Theoretical Physics, JINR.

Preprint of the Joint Institute for Nuclear Research. Dubna, 2003

Макет *Т. Е. Попеко*

Подписано в печать 16.06.2003.
Формат 60 × 90/16. Бумага офсетная. Печать офсетная.
Усл. печ. л. 2,43. Уч.-изд. л. 3,67. Тираж 415 экз. Заказ № 53954.

Издательский отдел Объединенного института ядерных исследований
141980, г. Дубна, Московская обл., ул. Жолио-Кюри, 6.
E-mail: publish@pds.jinr.ru
www.jinr.ru/publish/